

**Evolution of fluid electrical conductivity (FEC) profiles associated  
with a contaminant plume in a horizontal single-plane fractured  
rock aquifer system**

**Malefa Florence Moleme**

**Student number: 2008013569**

*Dissertation submitted in fulfilment of the requirements in respect of the Master's Degree  
qualification MSc (Geohydrology) at the Institute for Groundwater Studies in the Faculty of  
Natural and Agricultural Sciences at the University of the Free State.*

Supervisor: Dr Modreck Gomo

July 2017



# DECLARATION

- (i) “I, Malefa Florence Moleme, declare that the Master’s Degree research dissertation that I herewith submit for the Master’s Degree qualification MSc (Geohydrology) at the University of the Free State, is my independent work and that I have not previously submitted it for a qualification at another institution of higher education.”
- (ii) “I, Malefa Florence Moleme, hereby declare that I am aware that the copyright is vested in the University of the Free State.”
- (iii) “I, Malefa Florence Moleme, hereby declare that all royalties as regards intellectual property that was developed during the course of and/or in connection with the study at the University of the Free State, will accrue to the University.”
- (iv) “I, Malefa Florence Moleme, hereby declare that I am aware that the research may only be published with the dean’s approval.”



.....

Malefa Florence Moleme

July 2017

## **ACKNOWLEDGEMENTS**

Immense gratitude is given to my supervisor, Dr Modreck Gomo for his tireless assistance, patience and fruitful discussions regarding the study, this work would have never been conceived without his invaluable contribution.

The National Research Foundation (NRF) and Water Research Commission (WRC) is sincerely thanked for funding this project, and the Institute for Groundwater Studies (IGS) is also thanked for providing the proper administrative facilities to undertake this study.

I would also like to extend my vast appreciation to my friends and colleagues Vhulenda Mandiwana, Mohau Mahantane, Phuti Seanego and Alberta Steyn for their generous assistance during the conducted laboratory experiments and field tests.

Finally, I whole-heartedly wish to thank my family for their immeasurable support throughout my academic career. A special thanks and appreciation to my parents, Molefi Joseph and Morakane Sina Moleme, who have been a great inspiration to me.

Above all, I thank the Almighty God for making everything possible.

## **KEYWORDS**

Aquifer; Borehole geophysics; Contaminant plume; Fluid electrical conductivity (FEC); Fracture; Groundwater flow; Horizontal single-plane fractured rock aquifer; Matrix.

# TABLE OF CONTENTS

DECLARATION .....	ii
ACKNOWLEDGEMENTS .....	iii
1 INTRODUCTION .....	1
1.1 Background .....	1
1.2 Aims and objectives .....	2
1.3 Significance of the research .....	3
2 LITERATURE REVIEW .....	4
2.1 Borehole geophysics .....	4
2.1.1 Types of borehole geophysical methods .....	4
2.1.2 Benefits and limitations of borehole geophysics profiling .....	16
2.2 Horizontal single-plane fractured rock aquifer system .....	17
2.2.1 Fracture hydraulic and mass transport characters .....	18
2.3 Laboratory models in groundwater investigations .....	25
2.3.1 Importance and limitations of groundwater models .....	25
3 LABORATORY EXPERIMENTS.....	27
3.1 Methods and materials .....	27
3.1.1 Design and construction of the physical model .....	27
3.1.2 Testing the performance of the physical model .....	29
3.1.3 FEC profiling .....	30
3.2 Results and discussion.....	30
3.2.1 Estimation of hydraulic and transport properties of the physical model .....	30
3.2.2 Assessing the performance of the physical model .....	34
3.2.3 Evolution of FEC profiles .....	38
4 FIELD EXPERIMENT .....	49
4.1 Description of the test site .....	49
4.1.1 Geology and Hydrogeology .....	50
4.1.2 Hydraulic and mass transport parameters .....	52
4.2 Methods and materials .....	53
4.3 Results and discussion.....	55
4.3.1 Background FEC profile .....	55
4.3.2 First arrival of plume FEC profile .....	56
4.3.3 Plume peak FEC profile .....	57

4.3.4	Residual plume FEC profile.....	58
4.3.5	Near background FEC profile.....	59
4.4	Study limitations .....	61
5	CONCLUSIONS AND RECOMMENDATIONS .....	62
5.1	Conclusions .....	62
5.1.1	Conceptual background profile.....	62
5.1.2	Conceptual elevated FEC profile .....	63
5.2	Recommendations .....	65
6	REFERENCES .....	67
	ABSTRACT.....	77

## LIST OF FIGURES

Figure 2-1 Contours of the neutron flux surrounding a point isotropic source in an infinite homogeneous rock medium (Adapted from IAEA, 1999).....	6
Figure 2-2 Contours of the neutron flux surrounding a point isotropic source located on the axis of a water filled borehole (IAEA, 1999).....	7
Figure 2-3 Typical electrical profiles for a sequence of sedimentary rocks (Repsold, 1989)....	8
Figure 2-4 Multi-echo acoustic tele-viewer log from a 125 mm diameter borehole with a 75 mm diameter plastic casing (Williams and Johnson, 2004). ....	10
Figure 2-5 Optical tele-viewer images of a 150 mm diameter borehole completed in sandstone (Williams and Johnson, 2004). ....	11
Figure 2-6 A typical FEC profiling assembly (Mohr and Smith, 2013).....	14
Figure 2-7 Examples of FEC profiles recorded in the field (Beauheim and Pedler, 2009)....	15
Figure 2-8 Zones of mobile and immobile water in a natural fracture (Raven et al., 1988). ..	21
Figure 2-9 Solute transport processes in fractured aquifer systems (Witthüser, 2001). ....	22
Figure 3-1 Schematic illustration of the horizontal single-plane fractured rock aquifer system physical model. ....	28
Figure 3-2 A picture showing the physical model of the horizontal single-plane horizontal fractured-rock aquifer system. ....	29
Figure 3-3 Results obtained from the tracer point dilution test. ....	32
Figure 3-4 Best fit between the simulated and the measured chloride tracer breakthrough concentration.....	34
Figure 3-5 Salt solute tracer breakthrough curves measured in the simulated borehole throughout a period of 280 mins.....	35
Figure 3-6 A comparison between horizontal single-plane fracture breakthrough curves obtained from the laboratory experiments with ones found in literature.....	37
Figure 3-7 FEC profile obtained under no flow conditions.....	38
Figure 3-8 The variation in electrical conductivity of different soils (Adapted from Grisso et al., 2009). ....	39
Figure 3-9 FEC values obtained under freshwater flow conditions. ....	40
Figure 3-10 Illustration of freshwater movement within the borehole. ....	41
Figure 3-11 Seawater intrusion mixing concept; less dense freshwater floats on top of denser saltwater (Henry, 1964). ....	42
Figure 3-12 FEC profile five mins after injection of the saline water.....	43

Figure 3-13 Arrival of the plume peak in the fracture was observed after 13 mins. ....	44
Figure 3-14 Profile obtained from a contaminated borehole in a fractured system located in Beaufort West town in South Africa (Gomo, 2009). ....	45
Figure 3-15 FEC profiles associated with the residual plume. ....	46
Figure 3-16 FEC profiles associated with near-background values. ....	47
Figure 3-17 Profiles showing three distinct zones; the upper diluted zone. ....	48
Figure 4-1 Plan view of some of the boreholes at the Campus Test Site. ....	50
Figure 4-2 Lithological logs of the injection borehole (UO3) and the monitoring borehole (CH2). ....	51
Figure 4-3 Schematic diagram of the different geological formations and aquifers present on the Campus Test Site (Botha and Cloot, 2004). ....	52
Figure 4-4 Average hydraulic conductivities (K) for the more prominent formations on the Campus Test Site as determined from double packer tests (Pacome, 2010). ....	53
Figure 4-5 Salt was introduced into the injection borehole using an injection sock which was tied to a rope. ....	54
Figure 4-6 The background FEC profile of (A) the field monitoring borehole (CH2) and (B) the laboratory monitoring borehole before the tracer was injected.. ....	56
Figure 4-7 The background profile versus the plume's first arrival profile (A) in the field and (B) in the laboratory. ....	57
Figure 4-8 FEC profile associated with the plume peak in (A) the field monitoring borehole and (B) the laboratory monitoring borehole.. ....	58
Figure 4-9 Profiles associated with the residual plume in (A) the field and (B) the laboratory.. ....	59
Figure 4-10 FEC profiles associated with near-background values (A) in the field and (B) in the laboratory.. ....	60
Figure 5-1 The background profile, which was observed under natural conditions (freshwater flow). ....	62
Figure 5-2 Profile associated with elevated FEC values; observed when a contaminant plume reached the monitoring borehole.. ....	64
Figure 5-3 The water towards the top of the fracture is more representative of aquifer water, whereas the water at the transition zone is a mixture of aquifer and lower- matrix water. ....	65



## **LIST OF TABLES**

Table 2-1 Geophysical profiling methods; their required borehole conditions and main objectives (Adapted from Wonik and Hinsby, 2006). .....	5
Table 3-1 The hydraulic conductivity of the fracture. ....	31
Table 3-2 Mass transport parameter estimates for the in a horizontal single-plane fractured rock aquifer system. ....	33

## LIST OF EQUATIONS

Equation 2-1: Hydraulic conductivity from Darcy's law (1856).....	18
Equation 2-2: Hydraulic conductivity of a saturated subsurface system (Bear, 1972).....	19
Equation 2-3: Solute transport in a fracture (Tang et al.,1981) .....	23
Equation 2-4: Solute transport in a matrix (Lever et al., 1985) .....	23
Equation 3-1: Darcy velocity (Drost et al., 1968).....	31
Equation 3-2: Converging radial flow with a pulse injection (Sauty, 1980) .....	32
Equation 3-3: Groundwater velocity (Sauty, 1980).....	33

## **LIST OF ABBREVIATIONS AND ACRONYMS**

**ATV:** Acoustic tele-viewer

**CEC:** Cation exchange capacity

**EMFM:** Electromagnetic flowmeters

**FEC:** Fluid Electrical Conductivity

**HPFM:** Heat-pulse flowmeter

**LNAPL:** Light non-aqueous phase liquids

**NaCl:** Sodium Chloride

**OTV:** Optical televiewer

**PVC:** Poly Vinyl Chloride

**REV:** Representative elementary volume

**TDS:** Total Dissolved Solids

**TLC:** Water Temperature Level and Conductivity meter

# 1 INTRODUCTION

## 1.1 Background

In hydrogeological investigations borehole profiling is an essential tool used for locating lithological changes, identifying water producing fractures at a detailed scale, evaluating groundwater quality and constructing regional or local geological models of groundwater reservoirs. Over the years, various borehole geophysical techniques have been developed to assist in the understanding of the subsurface environment and the compilation of site-specific conceptual models (Repsold, 1989; Mares and Kelly, 1994; Jorgensen and Petricola, 1995; National Research Council, 1996; Wonik and Hinsby, 2006). Among these methods is the fluid electrical conductivity (FEC) profiling method.

FEC profiling is a simple and efficient technique used to determine properties such as flow rate, salinity and hydraulic characteristics such as transmissivity (Doughty *et al.*, 2013). The method is also commonly used to identify and locate high inflow zones intersected by a wellbore, from which groundwater samples can be collected for the purpose of water quality monitoring (Gomo and Vermeulen, 2015; Gomo *et al.*, 2017). Moreover, the identified inflow zones may be targeted for transport and hydraulic tests which may assist in the understanding of groundwater flow and solute mass transport properties of the subsurface (Xu *et al.*, 1997).

The method primarily involves profiling the FEC with depth in a borehole under either natural or stressed conditions, using a downhole Temperature Level Conductivity (TLC) probe. Once the FEC tests are performed, observations may be derived from the obtained profiles. Zones where fluid flows through the borehole display anomalies in the FEC profiles, which may be analysed to infer inflow rate and salinity of the individual fractures (Doughty and Tsang, 2002; Doughty *et al.*, 2008).

The application of the FEC profiling method is generally limited to fractured rock aquifers (Doughty and Tsang, 2005). Fractured zones are of great interest in contaminant studies, mainly because they often provide the only permeable flow paths in otherwise impermeable rocks. Some of the studies which have applied the FEC profiling method in fractured rock aquifer systems include Doughty and Tsang (2005), Kurikami *et al.* (2008), Gomo (2009), Pacome (2010) and Doughty *et al.* (2013).

Despite the usefulness and efficiency of this method, the main challenge with its application is that it has not yet been studied under a controlled laboratory aquifer environment, in order to understand the typical FEC profile responses in aquifers of different structures and groundwater qualities. Furthermore, no guidelines have been developed to assist in the interpretation of FEC profiles under diverse hydrochemical conditions. As a result, the profiles are being interpreted with partial understanding which has often led to immense contradictions and confusion. For example, anomalies in FEC readings have been attributed to factors such as leaks (contamination) or evaporation of water (Michalski, 2007; Beauheim and Pedler, 2009), and a decrease in FEC readings has been attributed to factors such as condensation of water droplets on the casing walls (Michalski, 2007) or decontamination due to the inflow of freshwater (Pacome, 2010). Although these assumptions are often made with very little or no substantial scientific evidence, up until now no experiment has been conducted under controlled conditions to actually confirm or revoke the probability of these assumptions or explain reasons behind the different shapes acquired from FEC profiles. There is therefore a need to improve the understanding and interpretation of borehole FEC profiles in different aquifers as influenced by different hydro-chemical conditions.

## **1.2 Aims and objectives**

This study aims to investigate the behaviour of FEC profiles associated with a contaminant plume in a horizontal single-plane fractured rock aquifer system, under both laboratory and field conditions. This is done to improve the interpretation of FEC profiles, by providing insight on their evolution and essentially producing a guideline which could be referred to during their interpretation.

This aim will be achieved through the following objectives:

- Designing and building a physical model representative of a horizontal single-plane fractured rock aquifer system.
- Testing the performance of the physical model in terms of its hydraulic and mass transport characteristics.
- Using the physical model to test, observe and develop borehole FEC profiles under controlled laboratory conditions.

- Conducting a field test in order to assess the practical applicability of the obtained laboratory FEC profiles.

### **1.3 Significance of the research**

The FEC profiling technique is commonly used to identify and locate groundwater flow zones, from which groundwater samples may be collected for the purpose of water quality monitoring. The location of flow zones is particularly important for groundwater sampling because it assists in acquiring representative aquifer water during sampling (Gomo and Vermeulen, 2015; Gomo *et al.*, 2017). The identified groundwater flow zones may also be targeted for hydraulic and tracer tests which are essential for the understanding of groundwater flow and mass transport properties of aquifers (Tsang *et al.*, 1990; Pedler *et al.*, 1990; Doughty and Tsang, 2000, 2002, and 2004; Doughty *et al.*, 2008; Kurikami *et al.*, 2008).

As its main outcome, this research expects to improve understanding on the application and interpretation of the FEC profiling method in a horizontal single-plane fractured rock aquifer system, the process of locating groundwater flow zones from FEC data, as well as the collection of groundwater samples which are representative of aquifer water. For the purpose of this study only the horizontal single-plane fractured rock aquifer system is being investigated as a starting point. However, the evolution of FEC profiles in other aquifer types and perhaps other groundwater contaminants also needs to be investigated in order to improve the general understanding across different aquifer systems.

## **2 LITERATURE REVIEW**

This chapter gives insight on some of the most important borehole geophysical methods employed in groundwater studies, their principles and application. As part of the literature review this chapter also discusses the hydraulic and mass transport characteristics of a horizontal single-plane fractured aquifer system, which is followed by a brief discussion on the importance and limitations of laboratory models in groundwater investigations.

### **2.1 Borehole geophysics**

Borehole geophysics includes all methods which make continuous profiles or point measurements at distinct depth stations in a borehole (Kobr *et al.*, 2005). The methods essentially involve measuring the physical, chemical and structural properties of penetrated geological formations usually using profiling tools which are lowered into a borehole. Over the years, the application of borehole geophysical methods has been extensively researched in various studies: geological investigations (Doveton and Prenskey, 1992), hydrogeological investigations (Repsold, 1989; Mares and Kelly, 1994; Jorgensen and Petricola, 1995), and environmental investigations (Keys, 1996; Krammer, 1997; Taylor *et al.*, 2010).

#### **2.1.1 Types of borehole geophysical methods**

Borehole geophysical methods are mainly differentiated based on their distinct principles. There are various types available, these include radioactivity (IAEA, 1999; Meyers, 1992), electrical (Maute, 1992; Spies, 1996), electromagnetic (Paillet and Pedler, 1996), acoustic (Paillet *et al.*, 1992), optical (Gochioco *et al.*, 2002) and fluid profiling methods (Evans, 1995; Beauheim *et al.*, 1997; Gebrekristos, 2007; Gomo, 2009). Table 2-1 summarises the above mentioned geophysical profiling methods, their required borehole conditions as well as their main objectives. This is followed by a brief discussion of the methods.

**Table 2-1 Geophysical profiling methods; their required borehole conditions and main objectives (Adapted from Wonik and Hinsby, 2006).**

<b>Log type</b>	<b>Specific log</b>	<b>Borehole Conditions</b>	<b>Information</b>
<b>Radioactivity</b>	<ul style="list-style-type: none"> <li>• Gamma-ray</li> <li>• Spectral ray</li> <li>• Gamma-gamma(density)</li> <li>• Neutron- neutron (porosity)</li> </ul>	Open and cased holes with or without fluid.	Lithology, density, porosity, calibration of surface geophysics.
<b>Electrical</b>	<ul style="list-style-type: none"> <li>• Self-potential</li> <li>• Resistivity</li> <li>• Focused resistivity</li> </ul>	Open or screened holes with fluid.	Lithology, calibration of surface geophysics, location of PVC screens.
<b>Electromagnetic</b>	<ul style="list-style-type: none"> <li>• Induction</li> <li>• Susceptibility</li> </ul>	Open and PVC cased holes with or without fluid.	Lithology, saline waters.
<b>Acoustic</b>	Sonic	Open holes with fluid.	Lithology (porosity).
<b>Optical</b>	<ul style="list-style-type: none"> <li>• Borehole camera</li> <li>• Optical borehole tele-viewer</li> </ul>	Open and cased holes with clear water.	Casing or borehole condition, caving, slope and aspect of fractures and layers.
<b>Fluid</b>	Water quality	Open and cased holes with fluid.	EC, temperature, pH, O <sub>2</sub> , NO <sub>3</sub> , Eh, total gas pressure.

### **2.1.1.1 Radioactivity profiling methods**

Radioactivity (also known as nuclear) profiling methods principally measure either the natural gamma radiation, the secondary gamma or the neutron radiation produced by a primary radiation source. A lengthily review on radioactivity profiling methods is given by Meyers (1992) and IAEA (1999).

The natural gamma-radiation measured with a gamma-ray profiling tool is from the natural <sup>40</sup>K in the ground and the isotopes of the uranium and thorium decay series. These isotopes occur naturally in clay, making it possible to distinguish between sand and clay layers and to estimate the clay content. Gamma-ray profiles can be made in dry and cased boreholes. The gamma-radiation emitted by the source is scattered by the atoms of the surrounding rock and may be partially adsorbed depending on the density of the rock (Compton effect). Some of the scattered radiation is deflected back to the detector and recorded. The porosity of the rock can be derived from the measured density of the rock if the densities of the rock matrix and the pore fluid are



known (Eisler *et al.*, 1971). Density and porosity are important parameters for assigning a lithology to the strata penetrated by the borehole.

A neutron-neutron tool contains a neutron source and one or more neutron detectors. The neutron source is either a neutron-emitting radioactive isotope (NN) or a neutron generator (INN). In an INN tool, an accelerated deuterium beam is directed at a tritium target to produce neutrons with an energy of about 14 mega electron-volts (MeV). These fast neutrons lose energy when they collide with the nuclei of the atoms of the surrounding rock and are registered by the detectors as thermal and/or epithermal neutrons (Schweitzer *et al.*, 1988). Because the energy transfer is the most effective when the neutrons collide with hydrogen nuclei, which have the same mass, the counting rate is inversely proportional to the water content and porosity of the rock. The neutron source and the detectors are separated by a neutron barrier (lead shield) to suppress direct radiation. The counting rate is calibrated with a material with a known porosity and is expressed as neutron porosity. Water content and the lithology of the rock can be derived from the neutron porosity values (Grau *et al.*, 1990).

In an ideal situation where the isotropic point neutron source is embedded in an infinite homogeneous medium, the spatial flux distribution of slowed-down neutrons has a perfect spherical symmetry as shown in Figure 2-1.

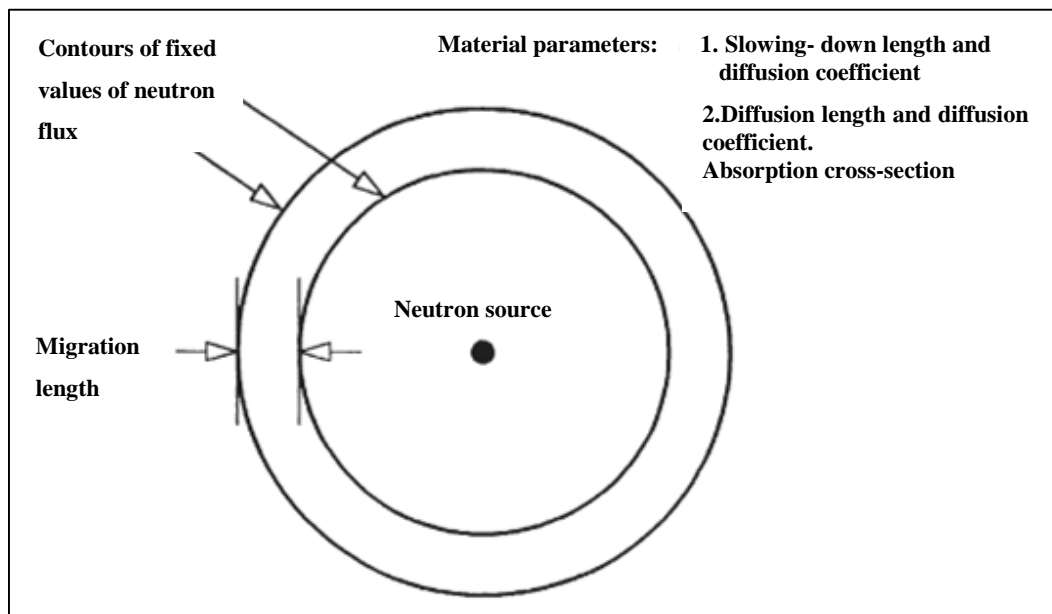


Figure 2-1 Contours of the neutron flux surrounding a point isotropic source in an infinite homogeneous rock medium (Adapted from IAEA, 1999).

However, when the same neutron source is placed at the axis of a borehole filled with water, the two spherical isoflux contours of the idealised situation displayed in Figure 2-1 become deformed as illustrated in Figure 2-2. This is because inside a borehole the two contours are much closer than in a formation. Therefore, the influence of the borehole itself needs to be corrected for by simultaneously measuring with two detectors at different distances from the source. The influence of the borehole on the measurement can be checked using a model with a known hydrogen content with the measurement expressed in water units (WU).

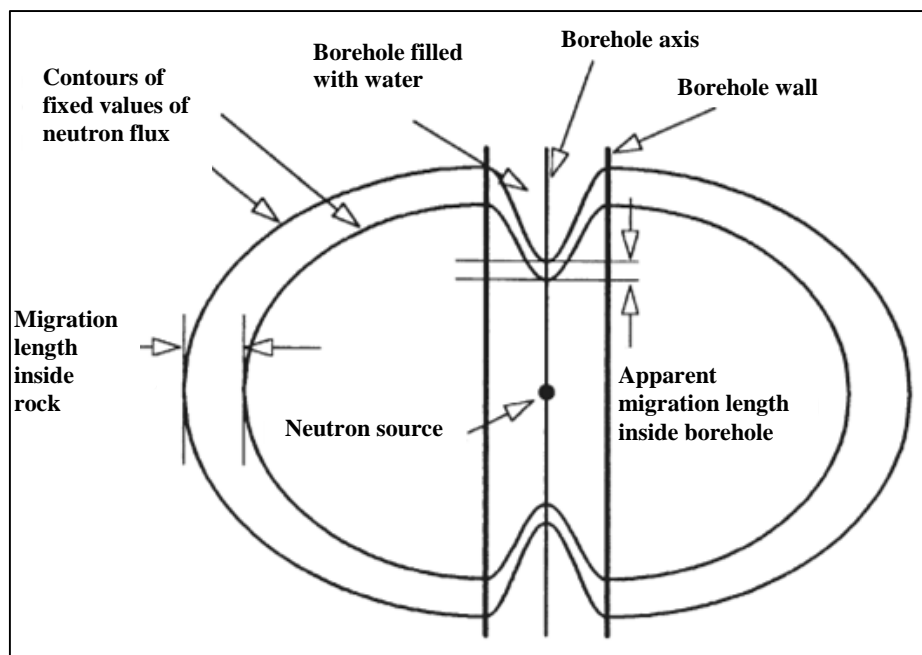


Figure 2-2 Contours of the neutron flux surrounding a point isotropic source located on the axis of a water filled borehole (IAEA, 1999).

### 2.1.1.2 Electrical profiling methods

Electrical profiling methods can only be employed within water or drilling fluid in a borehole. They are used in open holes to determine the electrical resistivity of the rock, which together with other physical parameters can be used to derive a lithological profile for the borehole (Ward, 1980; Maute, 1992; Spies, 1996). Some electrical borehole profiling tools measure the self-potential, while others measure the resistivity using one of numerous electrode configurations.

A self-potential tool (SP) measures the natural electrical potential between an electrode at the ground surface and an electrode in a drilling-fluid-filled borehole. This natural potential is caused by electrochemical processes occurring between different fluids. A prerequisite for an

interpretable SP profile is a clear difference between the resistivity of the drilling fluid and the formation pore water, together with an alternating sand/clay sequence with a distinct difference between the potentials of the sand and clay layers. The acquired change in potential with depth is then plotted (Maute, 1992).

In conventional resistivity profiling (electric log and micro-log), the resistivity of the rock is measured using a four-electrode array analogous to direct current (DC) resistivity surveys at the ground surface. A constant current is introduced into the rock between two current electrodes in the profiling tool. The potential measured between two other electrodes (potential electrodes) is proportional to the electrical resistivity of the rock. The measured value is called the “apparent resistivity” and is dependent on the size of the borehole, the adjacent rock, the overlying rock as well as the underlying rock. The “true” resistivity of the rock can be derived from the apparent resistivity using master curves. Other electrical borehole profiling probes include the later-log (focused electro-log) and the dip-meter tool (Spies, 1996). Typical electrical profiles from a sedimentary sequence are illustrated in Figure 2-3.

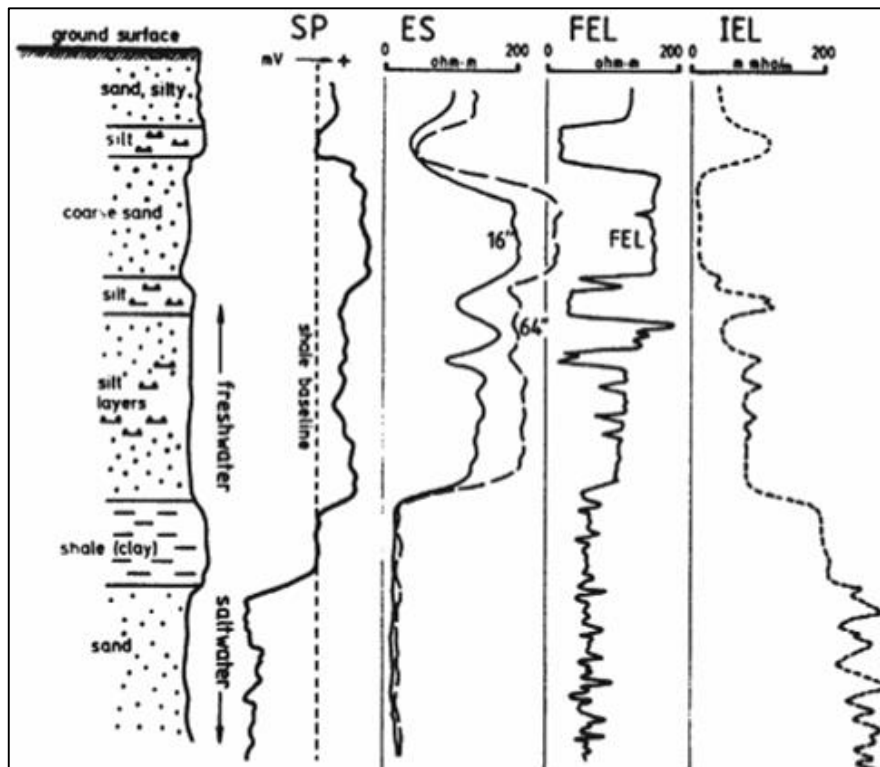


Figure 2-3 Typical electrical profiles for a sequence of sedimentary rocks. SP: self-potential profile; ES: electric profile 16- and 64- inch normal; FEL: focused electric log; IEL: induction log (Repsold, 1989).

### **2.1.1.3 Electromagnetic profiling methods**

Electromagnetic borehole profiling methods can be used in both dry and fluid-filled boreholes. In contrast to electrical methods, these methods can also be used in boreholes with plastic casing. Parameters such as electrical conductivity (EC) and susceptibility can be determined using an induction tool or a susceptibility tool, respectively. Both parameters can be used for lithological classification of the rock sequence (Maute, 1992; Smits *et al.*, 1993; Spies, 1996).

When using an induction tool to determine the electrical conductivity/resistivity of the rock surrounding a borehole, a transmitter coil is typically used to generate an alternating magnetic field around the borehole, which in turn induces electrical eddy currents that are proportional to the conductivity of the rock. An induction tool usually contains two coil systems with different coil spacing and therefore different investigation depths (Maute, 1992). The investigation depth depends on the conductivity of the rock. If the difference in the conductivities is large, the resistivity curve recorded by focused systems overshoots the proper value when the profiling tool passes the layer interface. In highly conductive rocks, the signal is weakened due to the skin effect. The same principles are used by a susceptibility tool (Wonik and Hinsby, 2006).

### **2.1.1.4 Acoustic profiling methods**

Acoustic borehole profiling tools comprise one or two ultrasound generators and several receivers in a linear array. The value for the ultrasound travel-time is an average for the distance between the transmitter and the receiver (s). Acoustic borehole profiling can only be conducted within water or drilling fluids in a borehole (Paillet *et al.*, 1992). They are generally conducted in open holes for lithological classification of the rock sequence, as well as for detecting joint and fracture zones. If the velocity in the rock matrix is known, the porosity of the rock can also be determined (Wonik and Hinsby, 2006). Increasing the distance between the ultrasound generator and the receiver, increases the investigation depth and decreases the vertical resolution. This method has been lengthily discussed by Paillet *et al.* (1992).

An acoustic image of the borehole wall can be produced with a borehole tele-viewer. A rotating sonic generator transmits 250 ultrasound pulses per rotation with 3 - 6 rotations per second. The travel-time and amplitude of the received signal is recorded and displayed in false colour to represent the borehole walls relative to north. The image generally has a high resolution thus allowing fractures, joints and fracture zones to be identified together with their spatial

orientation (Williams and Johnson, 2004). Acoustic tele-viewer (ATV) images can be collected in water-or light mud-filled intervals of boreholes. Borehole enlargements related to structures such as fractures, foliation and bedding planes scatters energy from the acoustic beam, reduces the signal amplitude and produces recognizable features on the images (Paillet *et al.*, 1990). Multi-echo systems which were first described by Broding (1982) measure the full wave train of the reflected acoustic signal and are capable of imaging behind plastic casing (Figure 2-4). Such systems are useful for imaging poorly competent intervals that will not stay open without being cased, and for inspecting annular grout seals (Williams and Johnson, 2004).

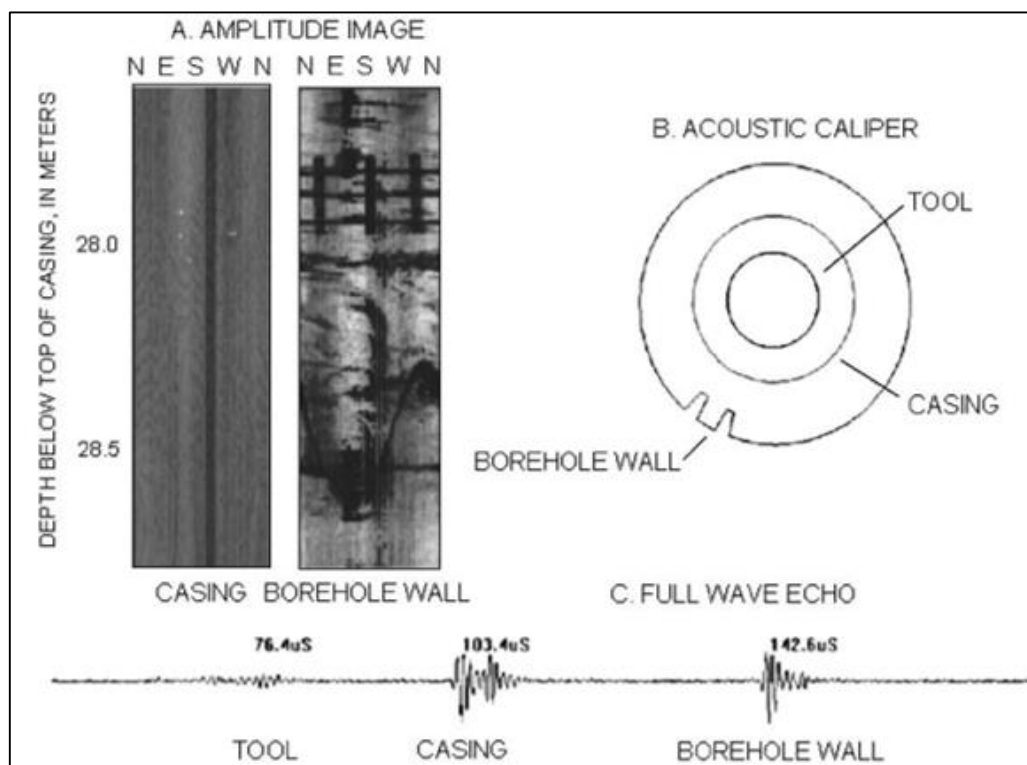


**Figure 2-4 Multi-echo acoustic tele-viewer log from a 125 mm diameter borehole with a 75 mm diameter plastic casing:** (A) Amplitude images of plastic casing and borehole wall behind the plastic casing (vertical and horizontal bands above 28 m are steel centralizers attached to the outside of the casing). (B) Cross-sectional view of an acoustic caliper. (C) Trace of the full wave echo (Williams and Johnson, 2004).

### 2.1.1.5 Optical profiling methods

An image of the borehole wall can be acquired directly by using a video camera, thus allowing for a qualitative assessment of the borehole wall or casing. However, the video camera can only be used in dry boreholes or in clear water, visibility is also dependent on the lens and the availability of light (Wonik and Hinsby, 2006). In air-percussion holes it may be beneficial to wet borehole walls above the water level to remove the dust left from drilling.

Optical tele-viewer (OTV) imaging systems uses a ring of lights to illuminate the borehole, a charge-coupled device (CCD) camera, and a conical or hyperbolic reflector housed in a transparent cylindrical window (Gochioco *et al.*, 2002). The length of the most commonly used OTV tools ranges from 1.4-2.8 m and 40-50 mm in diameter. The CCD camera measures the intensity of the colour spectrum in red, green, and blue. The reflector focuses a 360° slice of the borehole wall on the camera lens. Light intensity is either preset before profiling or in some systems may be adjusted while profiling (William and Johnson, 2004). Depending on the probe used, the optical image scan can either be sent up the profiling cable as an analogous signal and then digitized uphole or digitized downhole and sent up as a digital signal. A comparison of images from uphole and downhole-digital, conical and hyperbolic reflector OTV systems is displayed in Figure 2-5. The maximum borehole diameter in which OTV images can be collected is typically 300 mm or less.

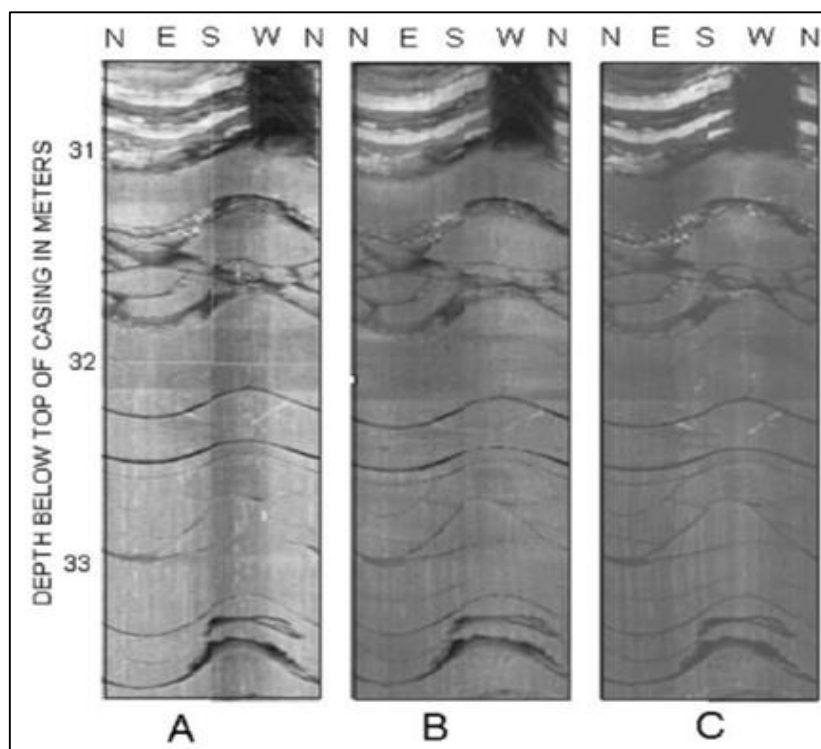


**Figure 2-5 Optical tele-viewer images of a 150 mm diameter borehole completed in sandstone: (A) Uphole-digital conical reflector. (B) Downhole-digital conical reflector. (C) Uphole-digital hyperbolic reflector (Williams and Johnson, 2004).**

Both the acoustic and optical images have their distinct advantages and should be employed based on the aim of the task. Fractures are more clearly defined under a wider range of conditions (i.e. dark-coloured rocks, cloudy borehole water and coated borehole walls) on

acoustic images than on optical images. However, optical images permit the direct viewing of the character as well as relation between lithology, fractures, foliation and bedding. The best approach is the combined application of both the acoustic and optical imaging with an integrated interpretation (Williams and Johnson, 2004).

#### **2.1.1.6 Fluid borehole profiling method**

Fluid borehole profiling methods can only be employed within water or a drilling fluid. When using this method, the temperature (TEMP) and electrical resistivity (SAL, for salinity) of the fluid is usually measured together with a single profiling tool (i.e. TLC probe). The measurements can either be taken as the probe is lowered into the borehole or as it is pulled upwards towards the surface (pull-up approach). Electrical resistivity cannot be measured above the groundwater table therefore it is easy to determine when the probe has entered the water (Wonik and Hinsby, 2006).

The combination of the TEMP and SAL profiles provide an indication of the vertical movement of water within the borehole. If the temperature of the surrounding rock undisturbed by the drilling process is needed, it is necessary to wait until the temperature has returned to its natural state. A multi-parameter probe may also be used to measure pH, oxygen concentration and redox potential of the fluid, which can assist in the monitoring of water quality (i.e. contamination). An example of a fluid profiling method is the fluid electrical conductivity technique.

##### **2.1.1.6.1 Fluid electrical conductivity (FEC) profiling method**

FEC profiling method is a simple and efficient method which has been widely used to locate conductive fracture zones as well as other hydraulic features that control water quality. It involves analysing the time-evolution of the FEC profiles obtained in a borehole under either natural or stressed conditions (Doughty and Tsang, 2004). The method was initially developed for the radioactive waste programme in Switzerland in the 1980s (Tsang *et al.*, 1990) and has since been applied in numerous studies both internationally and locally (Beauheim *et al.*, 1997; Gebrekristos, 2007; Gomo, 2009; Pacome, 2010).

###### **2.1.1.6.1.1 Definition of FEC**

Fluid electrical conductivity, which may also be referred to as specific conductance (conductance of water at 25 °C) is a measure of the ease with which electrical current can pass

through a fluid. It has the System International (SI) unit of Siemens per meter ( $S \cdot m^{-1}$ ). However, since natural water (i.e. groundwater, surface water, rain water) generally has low conductivity values, sub-multiples of  $S \cdot m^{-1}$  such as micro-Siemens per centimetre ( $\mu S \cdot cm^{-1}$ ) or milli-Siemens per meter ( $mS \cdot m^{-1}$ ) are commonly used (Pacome, 2010).

The conductivity of fluid generally depends on its ionic strength (concentration of charged ions) and the ability of these ions to move. The electrical conductivity (EC) of a material (i.e. water) increases with the increasing impurity within the material (Pacome, 2010); pure water has a very low conductivity and may thus be regarded as a non-conductor. Therefore, EC may provide useful indications of changes in the composition of water, mainly its total dissolved ions (McNeely *et al.*, 1979).

#### **2.1.1.6.1.2 Basic FEC principles for aquifer (borehole) flow and transport processes**

The FEC profiling method essentially entails profiling the FEC of a system over the length of the borehole column with an electrical conductivity probe in order to identify the locations where the water is flowing in or out of the borehole (Tsang and Doughty, 2003). The changes in FEC observed during profiling reflect the combined effects of two factors; (1) The magnitude of the flow (which is directly related to transmissivity and hydraulic gradient) and (2) the electrical conductivity of the flowing water. Without the measurements of the fluid's EC and an estimate of the hydraulic gradient, changes in FEC cannot be directly related to transmissivity (Beauheim and Pedler, 2009).

FEC profiling may be conducted under natural flow or stressed conditions (low pumping rate) as well as on natural or altered borehole water. In addition to its ability to identify contrasting features related to water salinity, FEC profiling may also be used as a measure of salinity for in situ determination of the effective diffusion matrix (Witthüser *et al.*, 2003), the porosity of the matrix (Gebrekristos, 2007) and Darcy's velocity at a fracture position (Gomo, 2009). Figure 2-6 displays a typical field assembly required for conducting FEC profiling as well as key dilution and hydraulic response processes which occur during the profiling.



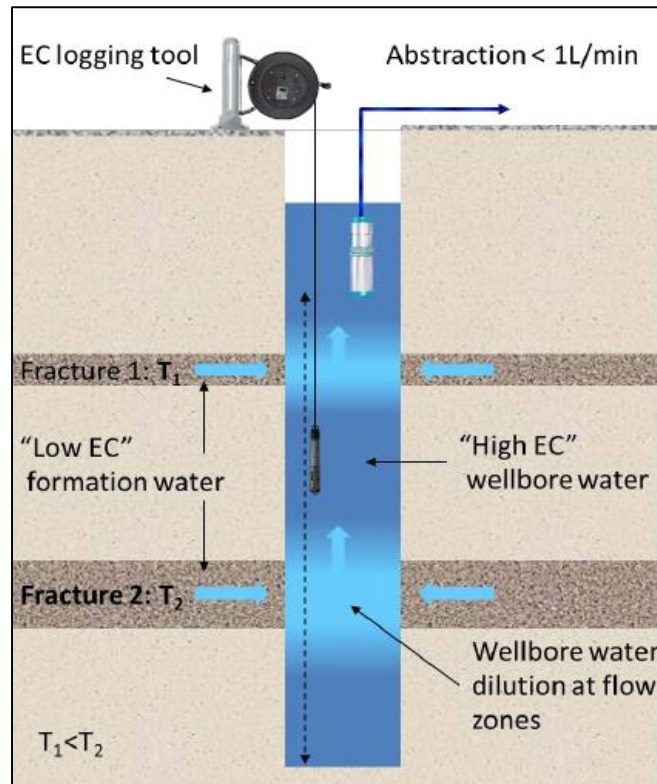


Figure 2-6 A typical FEC profiling assembly (Mohr and Smith, 2013).

Further details on the principles of the FEC method can be found in Tsang *et al.* (1990), Tsang and Doughty (2003), Doughty and Tsang (2005), and Doughty *et al.* (2005).

### 2.1.1.6.1.3 Application and interpretation of the FEC profiling

FEC profiling has been utilised by Tsang *et al.* (1990), Pedler *et al.* (1990), Doughty and Tsang (2000), (2002) and (2005), Kurikami *et al.* (2008) and Gomo (2009). These investigations applied the method to determine fracture positions, transmissive zones, flow direction and fracture contributions. The early development and application of the method was done by Tsang *et al.* (1990).

A lot of the FEC profiling anomalies have been attributed to flow into the borehole, evaporation and lithological formations, often times with no substantial scientific confirmation. Figure 2-7 shows smoothed FEC profiles recorded by Beauheim and Pedler (2009). In Figure 2-7A two main peaks can be observed at approximately 323 m and a broad one in Figure 2-7B at approximately 372 to 377 meters below ground surface (mbgs); these peaks were attributed to highly permeable lithological formations. Whereas the peaks seen in Figure 2-7C (at approximately 322 m, 373 m and 443 mbgs) were attributed to flow into the borehole, Beauheim and Pedler (2009) further pointed out that the magnitude of these peaks cannot be

presumed to be directly related to the amount of inflow at each location because the FEC of the formation water entering the borehole at one depth is not necessarily the same as that of the water from a different formation entering at a different depth.

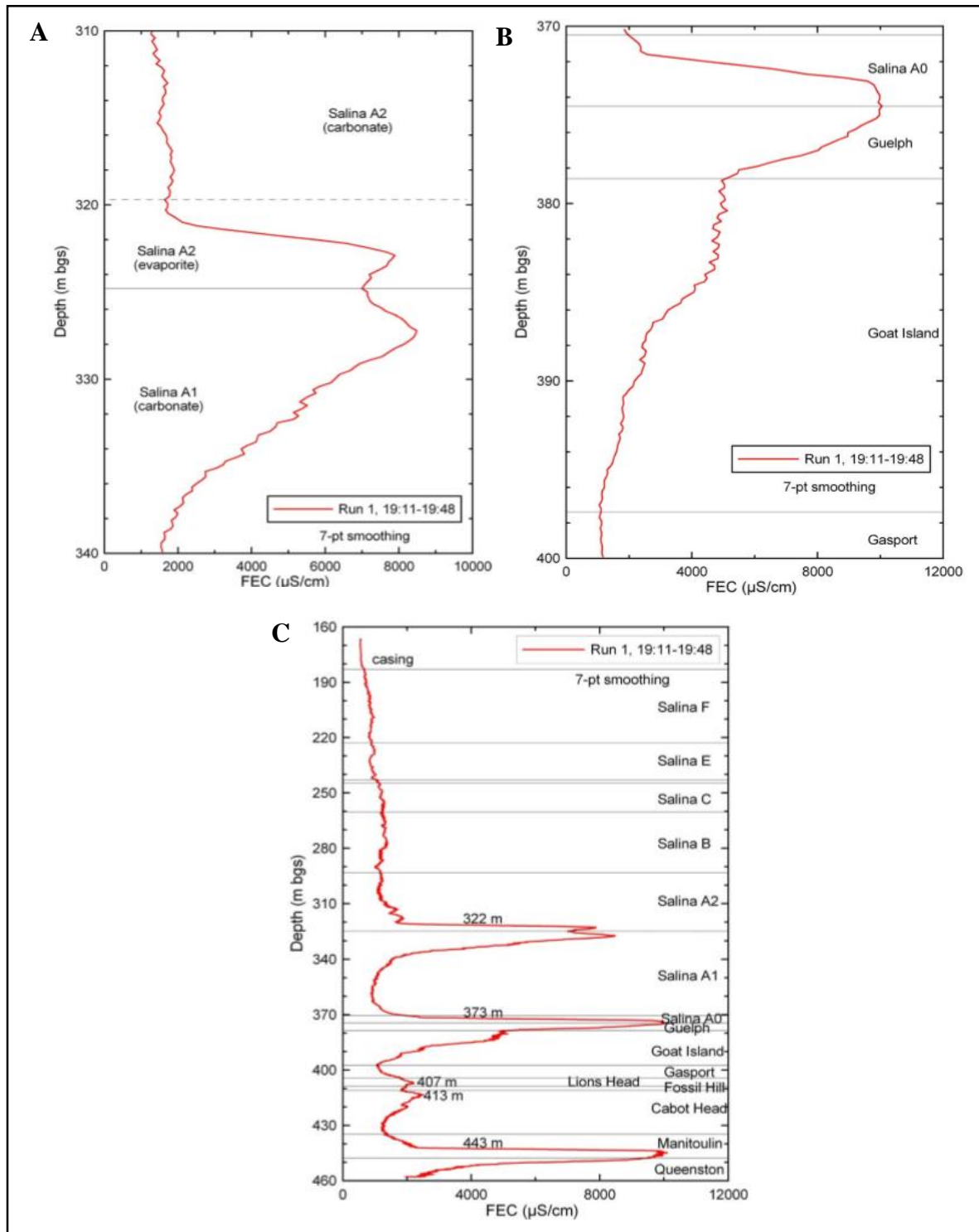


Figure 2-7 Examples of FEC profiles recorded in the field. The peaks observed in A and B are attributed to highly permeable lithological formations, whereas C is attributed to inflow into the borehole column (Beauheim and Pedler, 2009).

#### **2.1.1.6.1.4 FEC profiling analytical tools**

The analysis of FEC data includes three main approaches: (1) direct fitting of the time series of FEC profiles with a numerical model (Tsang *et al.*, 1990), which yields to the locations, inflow strengths and salinity of permeable features; (2) The mass integral method (Doughty and Tsang, 2005), whereby each profile is integrated over the entire profiled interval to provide an estimate of salt mass in place as a function of time, which can provide useful constraints on the direct fitting process; (3) Multi-rate FEC analysis (Tsang and Doughty, 2003), which enables transmissivities and hydraulic heads of the different permeable features to be determined.

Additionally, Doughty and Tsang (2000) developed a computer programme called BORE II, which is an enhanced version of BORE I (Hale and Tsang, 1988). This model can calculate the evolution of fluid electrical conductivity profiles in a wellbore or wellbore section, which may be pumped at a low rate and compares model results to log data in a variety of ways. BORE II broadens the range of applicability of the analytical solutions by considering multiple inflow and outflow feed points, isolated and overlapping FEC peaks, early-time and late-time behaviour, time-varying feed-point strengths and concentrations, and the interplay of advection and dispersion in the wellbore (Doughty and Tsang, 2005).

These methods are however limited to wellbore sections comprising only inflow points. Hence, they are not applicable to cases of horizontal flow across the wellbore diameter, internal wellbore flow and/or two manifestations of the co-existence of inflow and outflow feed points. Simply extending Evans' (1995) automated search method to systems which include both inflow and outflow feed points could prove challenging because the outflow feed points do not yield a direct effect on the FEC profiles.

#### **2.1.2 Benefits and limitations of borehole geophysics profiling**

The main objective of borehole geophysics profiling is to obtain information that cannot be acquired from conventional drilling, sampling and testing techniques. Drilling a borehole is an expensive procedure, but the borehole provides access to the subsurface for geophysical probes. Profiles may be interpreted in terms of lithology, thickness and continuity of aquifers, porosity, bulk density, resistivity, moisture content, groundwater chemical and physical characteristics, parameters of the water movement and the integrity of well construction (Wonik and Hinsby, 2006).

Profiling data can readily be reproduced over long periods, its repeatability and comparability provides the basis for measuring changes in yields of water wells with time. Thus, profiles may be used to establish baseline aquifer characteristics to determine the extent of changes from that baseline or to identify the movement of contaminant plumes through networks of observation boreholes. Unlike in sampling, whereby samples of fluid from a borehole provide data only from the sampled depth intervals and only after laboratory analysis, borehole profiles provide continuous recordings that can be analysed in real time at the well site (Keys, 1996).

However, geophysical borehole profiling cannot entirely replace sampling. A profile analyst cannot precisely evaluate a set of profiles without information on the local geological and hydrological conditions. To make the most of the results obtained from borehole profiling, at least one core hole should be drilled at each study site. Correct interpretation of profiles should be based on a thorough understanding of the operating principles of each profiling technique. Geophysical profiles can be analysed in the field to guide the location and frequency of sampling, and thus may reduce the number of samples needed along with the cost of sample processing and equipment decontamination (Wonik and Hinsby, 2006).

## **2.2 Horizontal single-plane fractured rock aquifer system**

A fracture is typically defined as a plane where there is barely any visible movement parallel to the surface of the fracture or else it is classified as a fault (Kruseman and de Ridder, 1994; Shapiro, 2002; Le Borgne *et al.*, 2007; Akoachere and van Tonder, 2009). Fractured rock aquifers are composed of a network of fractures that cut through a rock matrix. Therefore, characterization of fractured rock aquifers requires information on both the nature of the fractures and the rock matrix. The development of fractures is critical for the availability and yield of groundwater, thus the productivity of the aquifer is highest at shallow levels (Nyende *et al.*, 2014). Although groundwater flow in fractured porous media mainly occurs through fractures, the water contained within these aquifers is stored within the matrix. This has significant consequences on the movement of contaminants and other dissolved substances. Regardless of the permeability of the matrix, diffusion will cause mixing of solutes in the water flowing through the fractures with those in the immobile water in the rock matrix and pockets of no-flow-through fractures (Grisak and Pickens, 1980; Abelin *et al.*, 1991; Reedy *et al.*, 1996; Tsang and Neretnieks, 1998; Xu *et al.*, 1997; Becker *et al.*, 1999; Witthüser, 2001; Bäumlé, 2003).

## 2.2.1 Fracture hydraulic and mass transport characters

Water and mass transport characters are often studied together because the processes of flow and mass transport are usually related. The hydraulic characters (i.e. transmissivity, hydraulic conductivity, storativity and effective porosity) generally control the flow behaviour under natural and stressed conditions. Whereas the transport characters (i.e. flow velocity, diffusion, dispersion, advection etc.) mostly control the movement of mass (i.e. rock particles or dissolved ions), and are important in groundwater studies or vulnerability and risk assessment of aquifers (Pacome, 2010). Contaminant transport predictions which are only based on hydraulic measurements are subject to large errors (Van Wyk, 1998).

### 2.2.1.1 Hydraulic characters

The hydraulic conductivity of aquifers varies depending on the sorting of channel deposit aquifer materials and the amount of confining material such as shale, silt and clay present in the deposits system (Gomo, 2011). The hydraulic properties of water-bearing formations are essential as they control their groundwater storage and transmissive characteristics. By considering Darcy's law, Gehrels and Gieske (2003) illustrated mathematically how flow in homogeneous and isotropic conditions is controlled by two hydrogeological properties, namely; storage coefficient (specific storage for unconfined systems) and transmissivity. These hydrogeological properties are a function of physical characteristics such as porosity, density, geometry and shape of the voids between the grains.

#### 2.2.1.1.1 Hydraulic conductivity

Hydraulic conductivity is a measure of a material's ability to transmit water when subjected to a hydraulic gradient. It is usually expressed in meters per day (m/d). From Darcy's (1856) equation for flow in porous media, hydraulic conductivity can be written as:

$$K = \frac{Q}{Ai}$$

*Equation 2-1*

Where:

Q = specific discharge [ $L^3 T^{-1}$ ]

K = hydraulic conductivity [ $LT^{-1}$ ]

A = the cross-sectional area to flow [L<sup>2</sup>]

i = hydraulic gradient [-]

While hydraulic conductivity determines the ability of fluid to flow through the matrix of a material under specified hydraulic gradient; the material's fluid retention characteristic determines the ability of the system to retain the fluid under specified pressure conditions. Hydraulic conductivity is dependent on grain size, structure of the matrix, fluid properties and the amount of fluid present in the matrix (saturation).

The important properties relevant to the solid matrix include pore size distribution, pore shape, tortuosity, specific surface and porosity (Bear, 1972). The important properties of the fluid include fluid density and viscosity. According to Bear (1972), the hydraulic conductivity (K) of a saturated subsurface system can be expressed as:

$$K = \frac{k\rho g}{\mu}$$

*Equation 2-2*

Where:

K = Hydraulic conductivity [LT<sup>-1</sup>]

k = Intrinsic permeability of the earth material [L<sup>2</sup>].

ρ = Fluid density [ML<sup>-3</sup>]

g = Gravitational acceleration [LT<sup>-2</sup>]

μ = Dynamic viscosity [ML<sup>-1</sup>T<sup>-1</sup>]

#### **2.2.1.1.2 Transmissivity**

Transmissivity is a hydraulic parameter which gives measure of the rate of flow under a hydraulic gradient through a cross section of a unit width over the whole saturated thickness of the aquifer (Kruseman and de Ridder, 1992). It is expressed as a product of the average hydraulic conductivity (K) and the saturated thickness of the aquifer (D). When dealing with contamination in fractured aquifers (either in investigation or scenario testing), the knowledge of transmissivity of the fracture zone is important in order to evaluate velocities or the extent

of contamination plumes, especially for advective flow (Pacome, 2010). The transmissivity of a fracture is expressed as the product of the fracture's hydraulic conductivity ( $K_f$ ) and the equivalent fracture aperture ( $b$ ); which may be directly or indirectly calculated or estimated from the thickness of the fracture zone ( $D_f$ ) and the intersection angle ( $\Theta$ ). Various hydraulic (i.e. flowmeter, packer) and tracer (i.e. FEC profiling, dilution) tests have been developed to accurately estimate the transmissivity of fracture zones (Molz and Young, 1993; Botha *et al.*, 1998; Doughty and Tsang, 2000).

#### **2.2.1.1.3 Storativity**

The storativity of a saturated confined aquifer of thickness  $D$  is equal to the volume of water released from storage per unit surface area of the aquifer per unit decline in the component of the hydraulic head normal to that surface (Kruseman and de Ridder, 1992). The storage capacity of a fractured rock system consists of both the matrix and the fracture storativity. Usually the storage capacity of a fracture is very small compared to that of the matrix and it is thus often neglected in regional aquifer studies, however the knowledge of the storage capacity of the fracture or fracture network is vital in contaminant and artificial recharge studies (Botha *et al.*, 1998).

#### **2.2.1.1.4 Effective porosity**

The effective porosity of a fracture is defined as the ratio of the total volume of interconnected voids in the aquifer that contribute to flow, to the total saturated volume of the aquifer (de Marsily, 1986). The concept of effective porosity suggests that not all the pores within a system participate in the flow of water. Generally, fine grained and poorly sorted material have a low effective porosity whereas coarse grained and well sorted material have a high effective porosity, this is due to the greater retention of water on account of inter-granular forces (Singhal and Gupta, 2010). Effective porosity is more important than total porosity in the estimation of the average velocity of groundwater as well as in contaminant transport studies.

#### **2.2.1.2 Mass transport in fractured aquifers**

Within the fractured system there are zones where water flows and zones where water is stagnant. Solutes typically diffuse from the flowing water zones into the stagnant water zones, and further into the rock matrix. This process is referred to as matrix diffusion and it is largely responsible for the storage of solutes within the matrix of aquifers (Maloszewski and Zuber,

1990). Various studies have been carried out to determine flow paths, flow velocities and the effect of matrix diffusion and channelling on contaminant transport (i.e. Abelin *et al.*, 1991; Tsang, 1991; Reedy *et al.*, 1996; Tsang and Neretnieks, 1998; Xu *et al.*, 1997; Becker *et al.*, 1999; Maloszewski *et al.*, 1999).

In tracer tests the influence of matrix diffusion was verified by using multiple tracers with different molecular weight and hence different diffusion coefficient. These tracers resulted in different tailings of the breakthrough curves (Jardine *et al.*, 1999; Becker and Shapiro, 2000). The tail of the breakthrough curve is of great importance in describing matrix diffusion. According to Haggerty *et al.* (2000) the slope of the tail contains information about the type of mass transfer (i.e. single-rate or multi-rate diffusion or first-order sorption). The behaviour of the early-time (peak) is mainly accounted for by advection and dispersion.

Raven *et al.* (1988) studied fluid transport through parallel plates with irregular walls. The study revealed that transport through rough fractures promoted the formation of zones along the edges of the fracture where the water is immobile; the fluids moved through mobile zones, whereas the solutes diffused into immobile zones. Some of the solute was stored in the immobile zones during the early part of solute transport and was released over time as the solute concentration in the mobile fluid decreased (Figure 2-8).

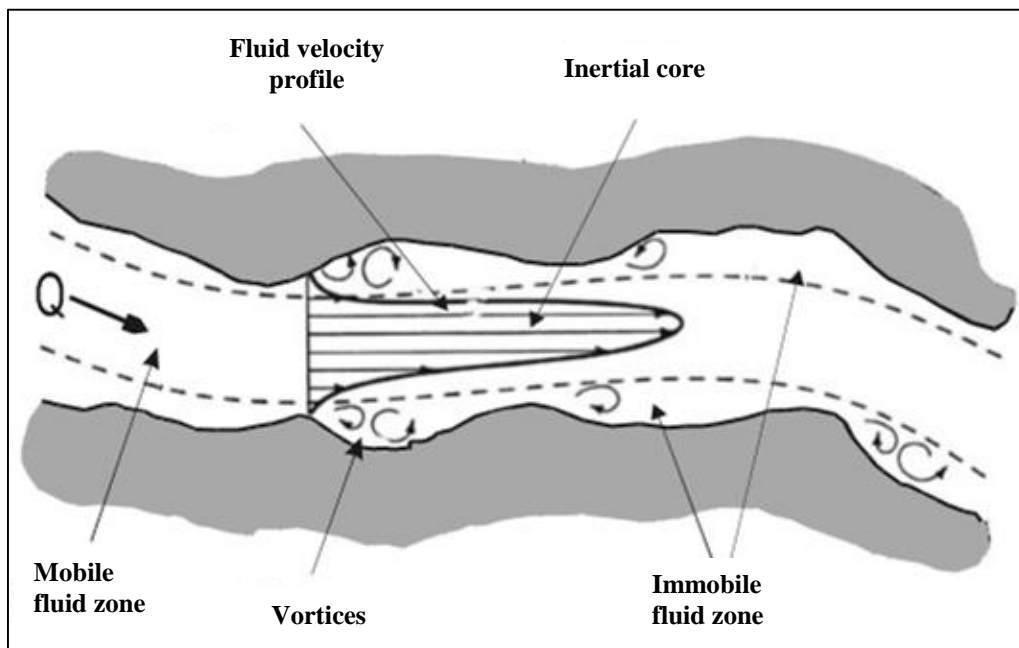


Figure 2-8 Zones of mobile and immobile water in a natural fracture (Raven *et al.*, 1988).



### 2.2.1.2.1 Transport processes in a single fracture

According to Zimmerman *et al.* (2002) during mass transport in fractures under laminar flow conditions the following will happen; the tracer will disperse both molecular diffusion perpendicular to flow as well as variation in the velocity profile across the fracture in the direction of the flow. The fluid closer to the walls will flow more slowly than the fluid in the aperture centre, as a result the tracer will advect with the fluid and spread longitudinally. This can cause a concentration gradient in the transverse direction that, in turn, causes diffusion towards the fracture walls into the matrix.

Mass transport processes in single fractured aquifer systems can be summarised as follows (Figure 2-9):

- Advection mainly at the mean fluid velocity in the fracture; the advection in the matrix is negligible due to the high contrast of permeability between fracture and matrix.
- Hydrodynamic dispersion in the fracture due to variations of local fluid velocities with respect to the mean velocity.
- Molecular diffusion in the fracture plane and from the fracture into the matrix.
- Physicochemical reactions between solute and the matrix and the fracture walls. These reactions cause retardation or slowing of apparent velocities.
- Biotic or microbial-mediated transformation.

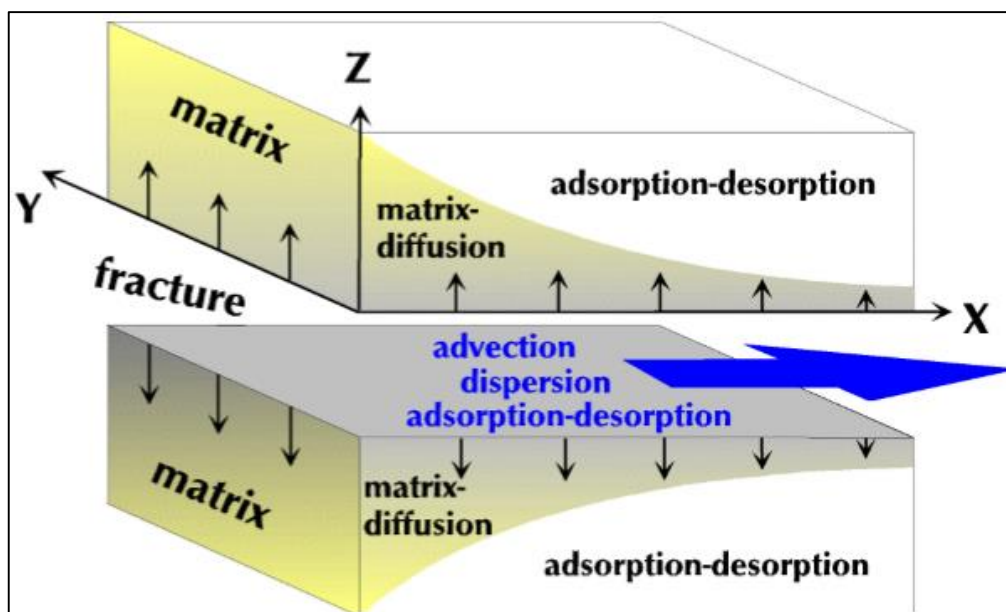


Figure 2-9 Solute transport processes in fractured aquifer systems (Witthüser, 2001).

The mathematical formulation of mass transport in fractured porous media has been given in various studies (Lee and Farmer, 1993; Sahimi, 1995; Becker and Shapiro, 2000; Witthüser *et al.*, 2003). The explanation of mass transport in fractured rocks with a porous matrix is governed by Equation 2-3 (Tang *et al.*, 1981) and Equation 2-4 (Lever *et al.*, 1985), which assumes that there is no advection in the rock matrix, the matrix is completely homogenous and isotropic and it extends infinitely away from the fracture. However, it is important to note that there are various other equations which can be used (e.g. Grisak and Pickens, 1980; Maloszewski and Zuber, 1985; Bear *et al.*, 1993) each equation takes into account the most dominant processes within a particular system.

The solute transport in a fracture is given by:

$$\underbrace{R_f \frac{\partial C_f}{\partial t}}_{\text{Retardation}} + \underbrace{\bar{v}_a \frac{\partial C_f}{\partial x_i}}_{\text{Advection}} - \underbrace{D_{h_{ij}} \frac{\partial^2 C_f}{\partial x_i^2}}_{\text{Dispersion}} - \underbrace{\frac{2D_e}{b} \cdot \frac{\partial C_p}{\partial z} \Big|_{z=\pm\frac{b}{2}}}_{\text{Diffusion}} + \underbrace{R_f C_f}_{\text{Decay}} = 0$$

Equation 2-3

Solute transport in the matrix is described by:

$$\underbrace{R_p \frac{\partial C_p}{\partial t}}_{\text{Retardation}} - \underbrace{\frac{D_e}{\varepsilon} \cdot \frac{\partial^2 C_p}{\partial z^2}}_{\text{Diffusion}} + \underbrace{R_p C_p}_{\text{Decay}} = 0$$

Equation 2-4

Where:

$R_f$  = Retardation coefficient of the fracture surface [-]

$R_p$  = Retardation coefficient of the rock matrix [-]

$C_f$  = Concentration in the mobile (fracture) zone [ML<sup>-3</sup>]

$C_p$  = Concentration in the immobile (matrix) zone [ML<sup>-3</sup>]

$\bar{v}_a$  = Average solute velocity in the fracture [LT<sup>-1</sup>]

$D_h$  = Hydrodynamic dispersion coefficient [L<sup>2</sup>T<sup>-1</sup>]

$D_e$  = Effective diffusion coefficient [L<sup>2</sup>T<sup>-1</sup>]

$b$  = Fracture width [L]

$i,j$  = Spatial coordinate direction  $x$  and  $z$  [-]

$x$  = Spatial coordinate taken to be positive in the direction of flow [-]

$z$  = Direction of transport in the matrix perpendicular to the fracture [-]

$\varepsilon$  = Effective porosity [-]

#### **2.2.1.2.1.1 Advection**

Advection describes the bulk movement of solutes along a mean direction of fluid flow, its rate equals the average interstitial fluid velocity/ linear pore fluid velocity (Kinzelbach, 1992). The velocity of the groundwater constitutes the velocity field for such transport. For practical reasons, this velocity field represents an average of different velocity fields over an appropriate volume. In a heterogeneous aquifer system, particularly in a fractured aquifer where the velocity field varies across the aperture of the fracture, along the fracture, and from one fracture to another, the averaged velocity field may not be representative of the small-scale field.

#### **2.2.1.2.1.2 Dispersion**

Dispersion describes the mixing and spreading of solutes along and transverse to the direction of flow due to local variations in interstitial fluid velocities. Dispersion is the transport process that controls the combined processes of spreading of mass solute that is not controlled by advection or diffusion. Solute flux due to mechanical dispersion can be described using Fick's first law, however this may lead to inaccurate consideration of dispersion (heterogeneity) in a fractured aquifer; where a solute must travel a certain distance before Fickian dispersion is established (Gelhar, 1986). Nicholl *et al.* (1999) illustrated the effect of fracture geometry on the dispersive transport.

#### **2.2.1.2.1.3 Diffusion**

Diffusion describes the solute transport which is driven by concentration gradients, however it may also occur in stagnant water. Molecular diffusion is caused by random molecular motion as a result of thermal kinetic energy of the solute. The molecular motion in liquids is smaller than in gases but greater than in solids. The coefficient of molecular diffusion is smaller for liquids in porous medium than in a pure liquid because a collision with the solids of

groundwater medium hinders diffusion (Schulze-Makuch, 2004). The value of the coefficient of molecular diffusion is dependent on the type of solute in the groundwater medium.

#### **2.2.1.2.1.4 Adsorption**

Adsorption describes the binding of molecules or particles to a surface due to their physical properties. In fractured systems such solutes may adsorb onto fractured surfaces; particularly in the presence of alteration products such as clay, and as a result be delayed in their movement. It is important to distinguish this process from the reversible matrix-fracture diffusion transport, which is mainly controlled by the physical properties of the aquifer (i.e. the porosity of the matrix, diffusivity of the matrix or the velocity of the solute in the fracture).

### **2.3 Laboratory models in groundwater investigations**

#### **2.3.1 Importance and limitations of groundwater models**

Groundwater models are extremely helpful in groundwater investigations. Anderson and Wang (1982) described a model as a tool designed to represent a simplified version of reality. In essence, a groundwater model provides a qualitative framework for synthesizing the field and for conceptualising hydrological processes (Anderson *et al.*, 2015). The organisation applied by a model helps the modeller to be aware of possible errors in assumptions and processes not previously considered.

Admittedly, the subsurface is highly heterogeneous and there is seldom enough data available to calibrate the model of an aquifer domain in a way that will completely accurately describe its heterogeneity. In contamination problems there is scarcely sufficient knowledge and data concerning all the chemicals and biological transformations that may take place (Bear and Cheng, 2010). Groundwater flow models often assume either a homogeneous porous media or a purely fractured media. Additionally, groundwater flow models in purely fractured systems often assume that the fractures are planar, parallel as well as identical (Akoachere and van Tonder, 2009). Although these assumptions are unlikely to be the reality, they provide a valuable starting point for understanding groundwater behaviour in fractured rocks. Therefore, groundwater models never uniquely represent the complexity of the natural world and have some level of uncertainty.

However, in view of all the uncertainties, a model's usefulness does not only rest on its ability to accurately predict the system's response; the model should also be employed for enhancing

understanding of various phenomena i.e. of flow and contaminant transport which takes place in it. By running a model of a given problem in a given domain, under various assumed conditions/scenarios, insight into the roles that various processes play in producing the system's response is gained.

In broad terms, groundwater models can be divided into physical (laboratory) models and mathematical models. Physical models include laboratory tanks and columns packed with porous material in which groundwater heads and flows are measured directly. For example, Darcy (1856) measured head in sand-packed columns of various diameters and lengths to show that flow in porous media is linearly related to the head-gradient. Usually, physical models are used at the laboratory scale (i.e. Mamer and Lowry, 2013; Illman *et al.*, 2012; Sawyer *et al.*, 2012; Fujinawa *et al.*, 2009).

Two types of mathematical models are considered; data-driven models and process-based models. Data-driven models use empirical or statistical equations derived from the available data to calculate an unknown variable from information about another variable that can be measured easily. Process-based models use processes and principles of physics to represent groundwater flow within the problem domain (Beven and Young, 2013). Mathematical models can be solved analytically or numerically. Mathematical models for groundwater flow are solved for the distribution of head in space and also in time for transient problems (Anderson *et al.*, 2015).

### **3 LABORATORY EXPERIMENTS**

This chapter gives a detailed description of the conducted laboratory experiments. Methods and materials are presented followed by a discussion of the results. The methods and materials section includes: the design and construction of the physical model representing the horizontal single-plane fractured rock aquifer system, testing of the model's performance and the application of the model to investigate FEC profiles associated with a contaminant plume. The term "contaminant plume" mentioned throughout this study refers to table salt (NaCl) used to represent saline conditions, and the term "profiling" may also be referred to as logging in other studies. After the methods and materials, the results and discussion sub-section is then presented; it comprises of the estimation of the model's hydraulic and mass transport properties, assessing the model's performance as well as its FEC profiling response.

#### **3.1 Methods and materials**

##### **3.1.1 Design and construction of the physical model**

Figure 3-1 is a schematic illustration of the physical model which was used to conduct tests in this study; it was designed to represent a typical horizontal single-plane fractured rock aquifer system. The physical model was 75 cm in length, 40 cm in height, 20 cm in width and the flow length was 55.5 cm long. The thickness of the aquifer itself was 26 cm. The groundwater flow was driven by the hydraulic gradient due to the difference in hydraulic heads between the inflow ( $H_1$ ) and ( $H_2$ ) the outflow points.

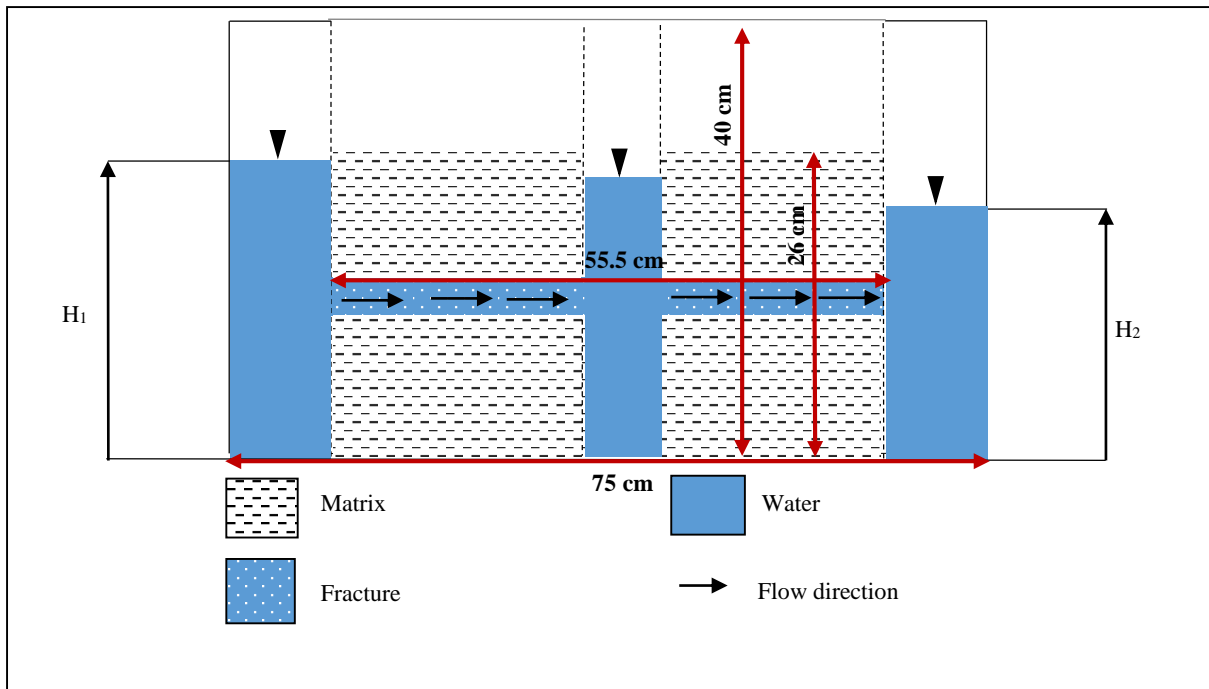


**Figure 3-1** Schematic illustration of the horizontal single-plane fractured rock aquifer system physical model. The model was 75 cm in length, 40 cm in height, 20 cm in width and the flow length was 55.5 cm long. The thickness of the aquifer itself was 26 cm.

An acrylic clear perspex material was used to construct the container into which soil material was placed, in order to form the different formations of the physical model. A poly vinyl chloride (PVC) pipe perforated throughout its entire length was used to represent a borehole, which was placed at the centre of the model. A 25 ℓ container was used to supply water into the model via the inflow section at a constant rate. Throughout the duration of the test, hydraulic heads of 25 cm (inflow) and 21 cm (outflow) above the base of the model were maintained in order to ensure a constant flow rate and hence constant discharge (Figure 3-2). For simplicity, clay soil was used to represent a low permeability matrix and coarse grained sand due to its exceptionally high hydraulic conductivity was used to represent the horizontal fracture.

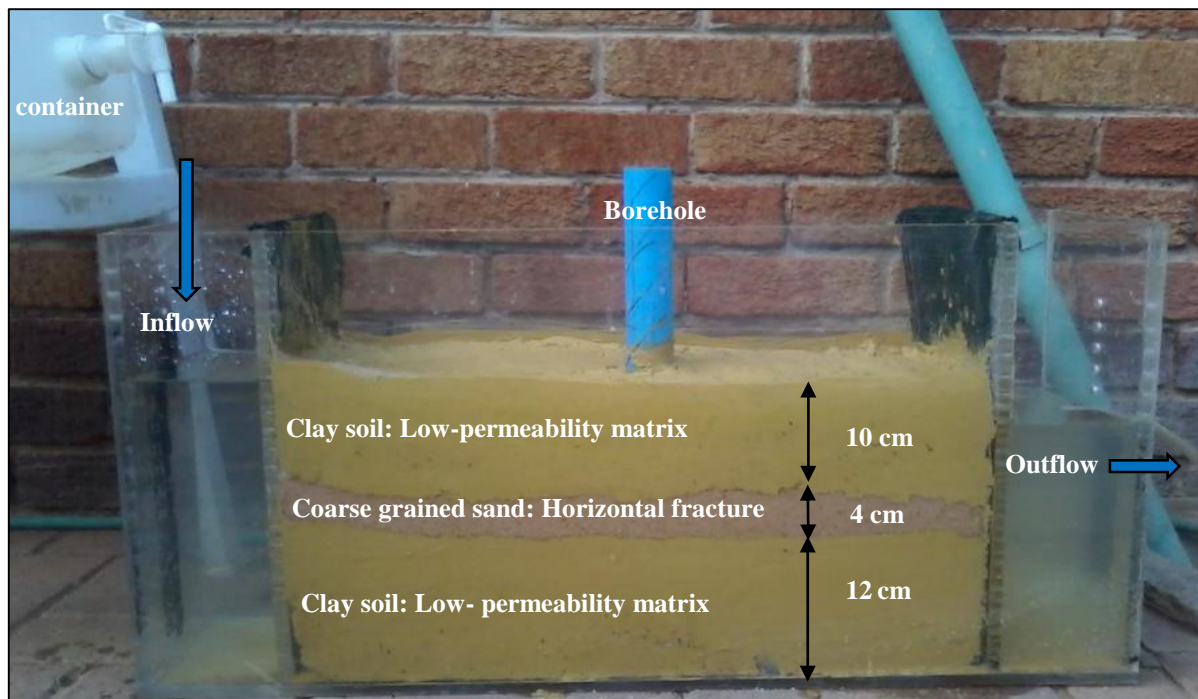


Figure 3-2 A picture showing the physical model of the horizontal single-plane horizontal fractured-rock aquifer system. Clay soil was used to represent the low permeability matrix and coarse grained sand was used to represent the horizontal fracture due to its exceptionally high hydraulic conductivity.

### 3.1.2 Testing the performance of the physical model

The performance of the physical model was tested by conducting tracer breakthrough tests and comparing the obtained breakthrough curves to the theoretical breakthrough curves of a typical horizontal single-plane fractured rock aquifer system. Another important reason for performing these tests was to obtain information of the tracer's average expected first arrival time, peak time and residual plume time in the monitoring borehole. This assisted with the FEC profiling procedure (i.e. profiling at the right time and interval) and ensured that the profiles associated with the above-mentioned stages were captured.

A TLC probe was used to record both FEC and head values within the borehole column, it was set to record readings every five seconds. The probe was attached to a string and placed inside the borehole with the sensor positioned at the fracture. Freshwater was run through the system for five mins, within this time background FEC measurements were recorded. Thereafter, 10 g of NaCl was diluted within a 500 ml jar of water and introduced into the system through the inflow side. Tracer movement in the system was monitored by measuring FEC in the monitoring borehole at constant intervals using the TLC probe.



The tracer breakthrough test was repeated twice and the obtained breakthrough curves were compared to the typical single-plane breakthrough curves found in literature, in order to show the capacity of the model to simulate mass-transport characteristics of a real system. As part of the characterisation of the physical model, a point dilution test was also conducted with the purpose of determining the Darcy velocity ( $q$ ) of the model.

### **3.1.3 FEC profiling**

After the capacity of the physical model to simulate mass-transport characteristics of the real system had been proven, the model was considered adequate to investigate the evolution of FEC profiles associated with a contaminant plume. The application of the FEC profiling technique was investigated using two different water quality scenarios; in freshwater and saline contaminated water. Normal tap water was used to simulate fresh groundwater flow and NaCl was added into the water to raise the FEC in order to represent a saline contaminated groundwater system. The tap water which was used to simulate an uncontaminated flow system had an average FEC of  $112 \mu\text{S}\cdot\text{cm}^{-1}$ .

Prior to contaminating the water with NaCl background FEC profiles were recorded within the borehole, these were used as indicators to identify and monitor the change within the simulated borehole column. Thereafter the water quality in the system was altered by adding NaCl; this alteration was achieved by mixing 10 g of salt within a 500 ml jar of water and then introducing it into the system through the inflow section of the model. After the saline water had been introduced into the system, there was a waiting period of four mins; according to the aforementioned tracer tests that was the time which the first arrival of the plume could be expected at the monitoring borehole. FEC profiling was then conducted by measuring the EC with depth (using a TLC probe) at uneven time intervals using a pull-up profiling protocol; negligible mixing is suspected while moving the TLC up and down to take measurements.

## **3.2 Results and discussion**

### **3.2.1 Estimation of hydraulic and transport properties of the physical model**

#### **3.2.1.1 Hydraulic Conductivity**

The hydraulic conductivity of the fracture was obtained by performing Darcy's experiment and the value of  $K$  was calculated using Equation 2-1 in Section 2.2.1.1.1 (Darcy, 1856). The test was conducted four times and an average value of 67.48 m/day was acquired (Table 3-1).

**Table 3-1 The hydraulic conductivity of the fracture.**

<b>Test no.</b>	<b>Q (m<sup>3</sup>/day)</b>	<b>A (m<sup>2</sup>)</b>	<b>i</b>	<b>K (m/day)</b>
<b>Test 1</b>	0.432	0.111	0.0721	53.98
<b>Test 2</b>	0.605	0.111	0.0721	75.60
<b>Test 3</b>	0.518	0.111	0.0721	64.72
<b>Test 4</b>	0.605	0.111	0.0721	75.60
<b>Average</b>	0.540	0.111	0.0721	<b>67.48</b>

### 3.2.1.2 Darcy's velocity

In this study a four cm fracture test section and a 10 g tracer were used. Under natural gradient conditions, tracer dilution in the test section is generally assumed to be due to the horizontal influx of fresh groundwater into the borehole test section. Assuming steady-state conditions and no density driven gradient, Darcy velocity was calculated using Equation 3-1 (Drost *et al.*, 1968) and a value of 1.01 m/day was obtained.

$$q = \frac{W}{\alpha A t} \ln \left( \frac{C_t}{C_0} \right)$$

*Equation 3-1*

Where:

W = volume of fluid contained in the test section [L<sup>3</sup>]

A = cross sectional area normal to the direction of flow [L<sup>2</sup>]

C<sub>0</sub> = tracer concentration at t = 0 [ML<sup>-3</sup>]

C<sub>t</sub> = tracer concentration at time = t [ML<sup>-3</sup>]

α = borehole distortion factor (between 0.5 and 4; = 2 for an open well. NOTE: qα = v\*, where v\* = apparent velocity inside the well)

t = time when concentration is equal to C [T]

Figure 3-3 shows FEC concentration with respect to time, it is evident that the tracer concentration decays (almost exponentially) with time.

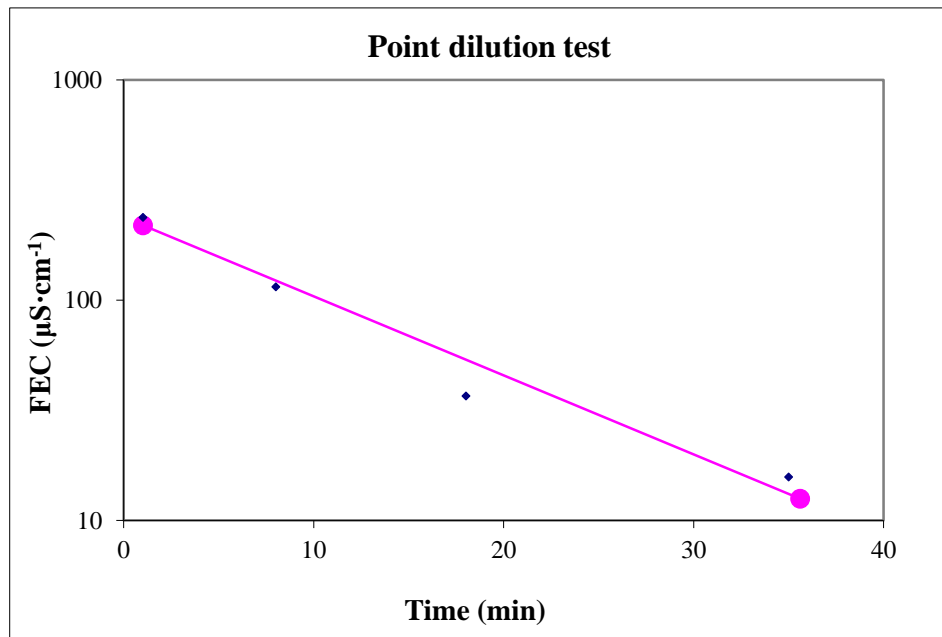


Figure 3-3 Results obtained from the tracer point dilution test.

### 3.2.1.3 Fracture transport parameters

Transport parameters such as groundwater velocity, dispersion and effective porosity were determined using the tracer breakthrough data. The values were quantified based on the approximate solution for converging radial flow with a pulse injection (Sauty, 1980):

$$c(r, t) = \frac{\Delta M}{2Q\sqrt{\pi \alpha_L vt^3}} \exp \left[ -\frac{(r - vt)^2}{4D_L t} \right]$$

Equation 3-2

Where:

$\Delta M$  = injected mass of tracer per unit section [ $ML^{-3}$ ]

$\alpha_L$  = longitudinal dispersivity [L]

$D_L$  = longitudinal-dispersion coefficient [ $L^2T^{-1}$ ]

$D_L = \alpha_L \times v$ ;  $v = v_f$ ; groundwater velocity under forced gradient [ $L^2T^{-1}$ ]

$Q$  = pumping rate of the well [ $L^3T^{-1}$ ]

$r$  = radial distance [ $L$ ] between the two boreholes

From Equation 3-2, the velocity and the effective porosity could be estimated from equation:

$$v = \frac{Q}{\varepsilon A}$$

*Equation 3-3*

Where:

$v$  = groundwater velocity [ $LT^{-1}$ ]

$Q$  = pumping rate of the well [ $L^3T^{-1}$ ]

$\varepsilon$  = effective porosity [-]

$A$  = cross sectional area normal to the direction of flow [ $L^2$ ]

Data was interpreted by fitting the theoretical model data to the measured Cl tracer breakthrough concentrations with the aid of the TRACER excel application (Riemann, 2002). On this TRACER excel application, manually changing the values of the dispersion and groundwater velocity until the simulated and measured data displayed a match yielded the estimates of the fitting parameters, which are displayed in Table 3-2.

**Table 3-2 Mass transport parameter estimates for the in a horizontal single-plane fractured rock aquifer system.**

<b>Distance between injection and observation point (m)</b>	<b>Mass of injected tracer (kg)</b>	<b>Dispersion (m)</b>	<b>Groundwater velocity (m/day)</b>	<b>Effective porosity</b>
0.2775	0.0046	0.3	20.19	0.05

The best match obtained between the simulated and measured data is presented in Figure 3-4.

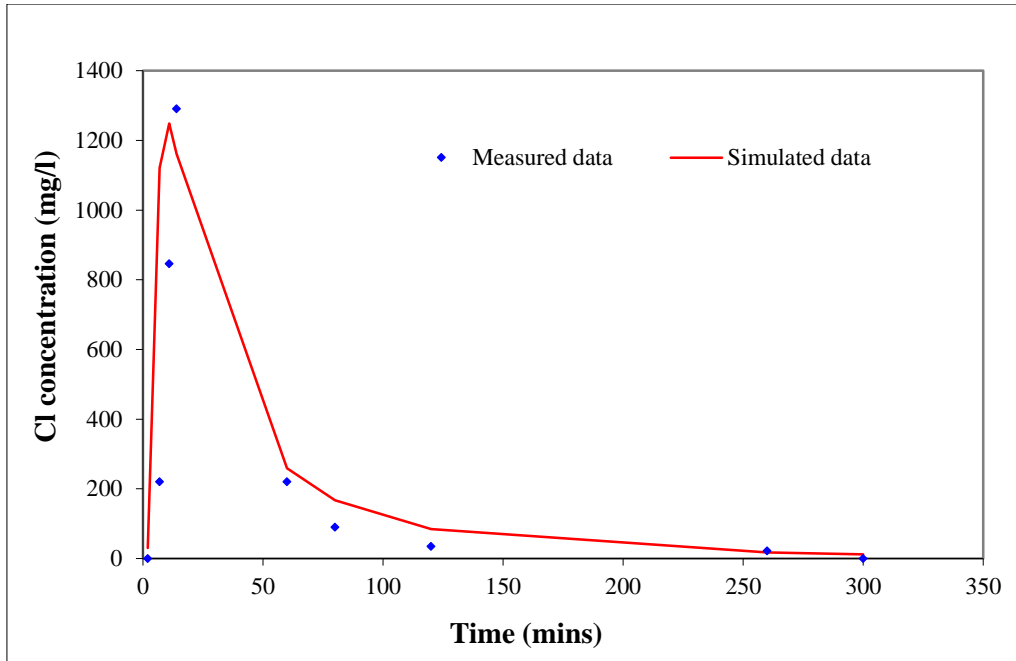


Figure 3-4 Best fit between the simulated and the measured chloride tracer breakthrough concentration.

### 3.2.2 Assessing the performance of the physical model

Figure 3-5 A and B show the tracer breakthrough curves obtained from measurements made in the simulated borehole over a period of 280 mins. The test was conducted twice and similar results were obtained. In the first test (Figure 3-5 A) the first arrival of the tracer was observed after four mins. A continuous increase was noted until a maximum peak of  $3960 \mu\text{S}\cdot\text{cm}^{-1}$  was reached after 12 mins. Thereafter the FEC started to decline as the peak of the tracer plume passed the monitoring borehole. In the second test (Figure 3-5 B) the tracer's first arrival was observed after five mins. An increase in FEC values was seen until a maximum peak of  $3532 \mu\text{S}\cdot\text{cm}^{-1}$  was reached after 16 mins. Thereafter, similarly to the first test, the FEC values started to decrease.

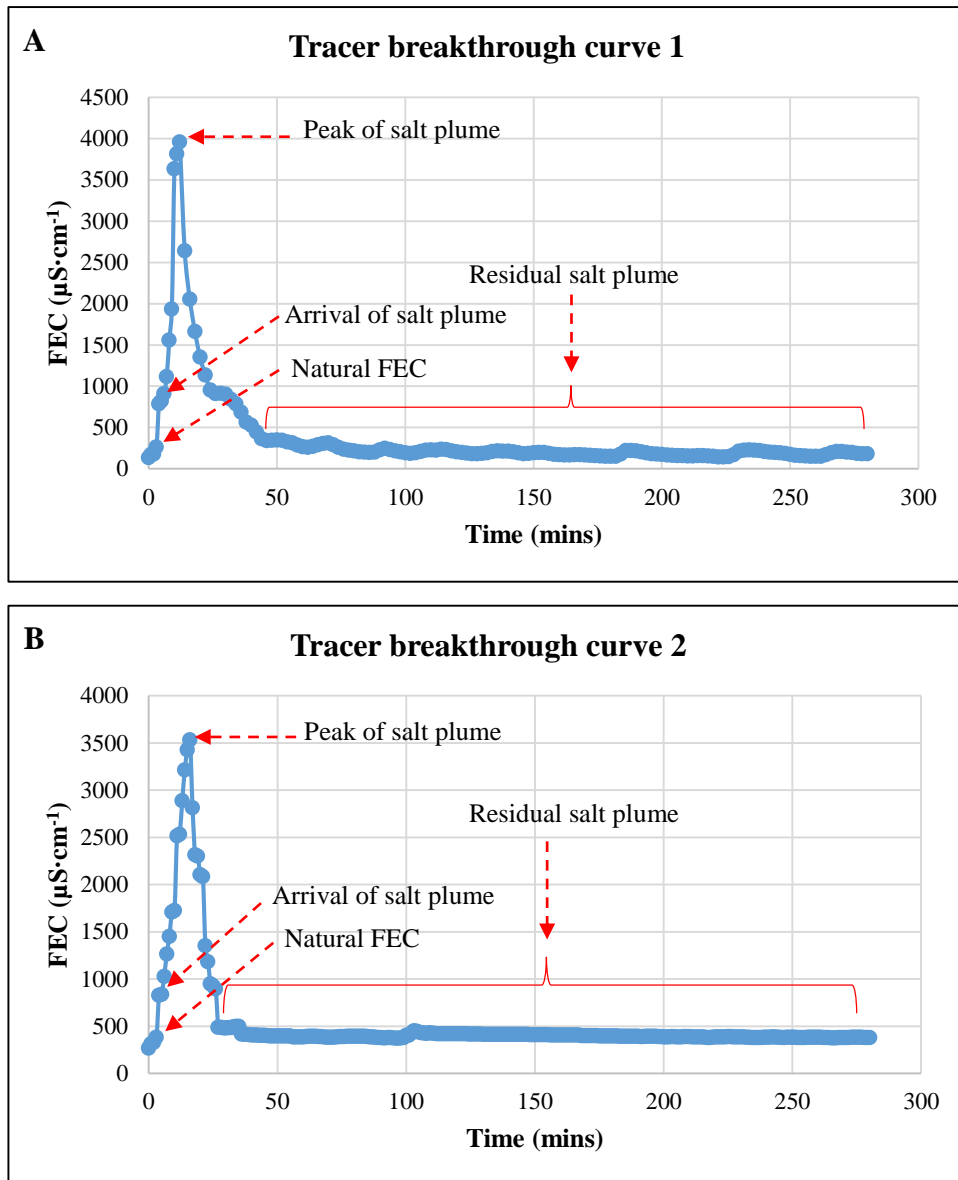


Figure 3-5 Salt solute tracer breakthrough curves measured in the simulated borehole throughout a period of 280 mins.

The general characteristics which can be noted from the tracer breakthrough curve results are that they are positively skewed; hence the peak time lies behind the mean tracer transit time. In addition, there is a rapid increase to the peak and then a long tail. The behaviour of the early-time (peak) is because most of the tracer moves through the fracture by the process of advection and dispersion, which is relatively faster (Zimmerman *et al.*, 2002). Whereas the other portion is delayed by the diffusion of the tracer into the matrix and/or into the stagnant zones in the fracture thus resulting in a long tail with low concentrations (Haggerty *et al.*, 2000).

The breakthrough curves obtained in the laboratory experiments were compared to the typical horizontal single-plane fractured rock aquifer breakthrough curves observed in literature

(Figure 3-6) in order to compare the extent of their similarities. These curves (from literature and the laboratory) were comparable in terms of their shape, early-time (peak) and long tail. The performance of the physical model was thus satisfactory and could therefore be used to test for FEC responses.

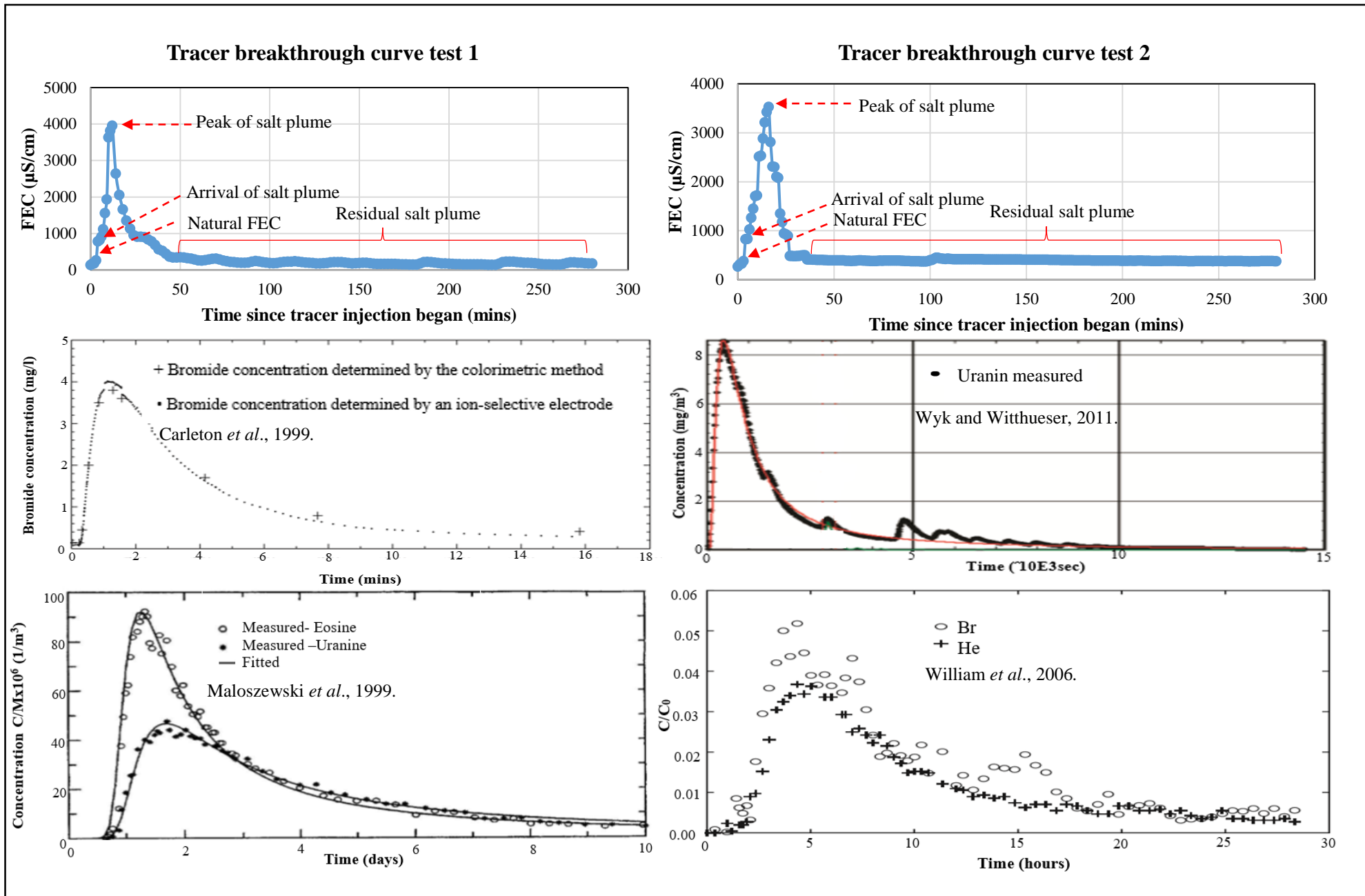


Figure 3-6 A comparison between horizontal single-plane fracture breakthrough curves obtained from the laboratory experiments with ones found in literature. The breakthrough curves were extremely comparable in terms of the positively skew shape, early-time (peak) and long tail. 37



### 3.2.3 Evolution of FEC profiles

This section presents and discusses results obtained from measurements recorded during the investigation of the evolution of FEC profiles. The first results presented are those observed under “no-flow” conditions. Thereafter, the background profiles obtained when freshwater was flowing in the system are discussed, followed by the FEC profiles associated with various stages of the contaminant plume (i.e. arrival of the plume, plume peak, residual plume profile and near background FEC profile). Throughout the entire discussion, the light blue shade represents the inflow zone (fracture position) and the light orange shade represents the low permeability matrix. The FEC of the tap-water throughout the duration of the experiment was measured to be  $112 \mu\text{S}\cdot\text{cm}^{-1}$ .

#### 3.2.3.1 FEC Profile during no-flow conditions

A background FEC profile was obtained under no-flow conditions in order to observe the natural FEC values of the soil material used (Figure 3-7). It can be noted that lower FEC values were recorded where the high permeability, low porosity coarse grained sand layer was located ( $118 \mu\text{S}\cdot\text{cm}^{-1}$ ), and slightly higher FEC values ( $135 \mu\text{S}\cdot\text{cm}^{-1}$ ) were obtained where the low permeability matrix was located; at the top and bottom section of the system.

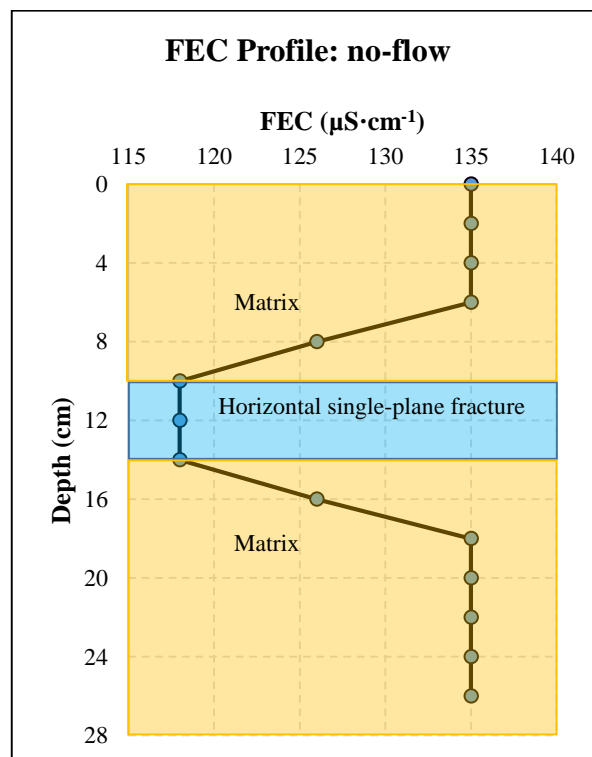


Figure 3-7 FEC profile obtained under no flow conditions. Coarse grained sand had an FEC value of  $118 \mu\text{S}\cdot\text{cm}^{-1}$  whereas the clay layer had a slightly higher FEC value of  $135 \mu\text{S}\cdot\text{cm}^{-1}$ .

These observations can be accounted for by the salts naturally found in the soil material (Figure 3-8). According to Grisso *et al.* (2009) the FEC of soils differs depending on the amount of moisture held by soil particles, which is a consequent of soil particle size and texture. FEC has also been shown to have a strong correlation to other soil properties such as cation exchange capacity (CEC), porosity and the drainage capacity of the soil. Therefore, on this basis sand generally has a low FEC, silt a medium one and clay has the highest FEC. No-flow conditions were maintained for 30 mins, thereafter freshwater was allowed to flow through the system.

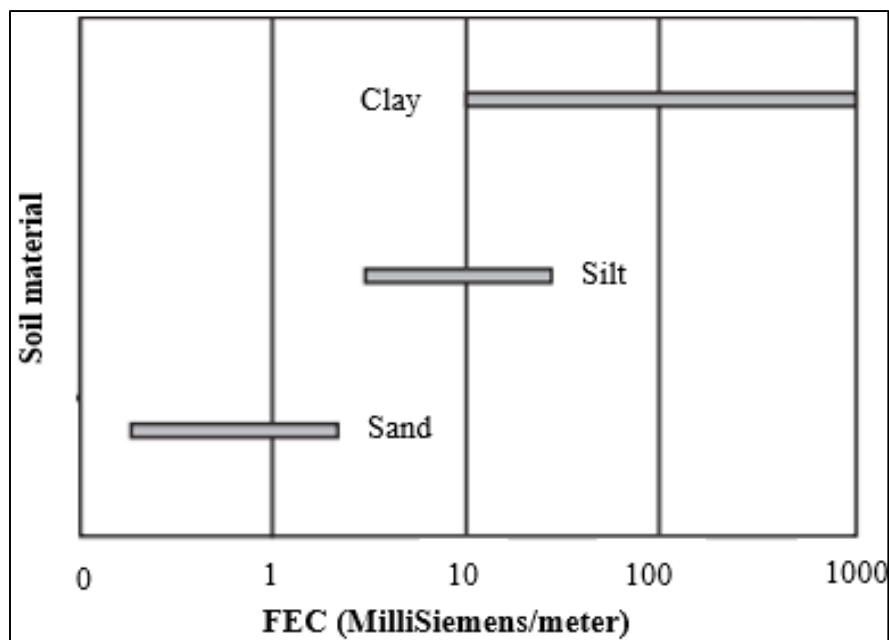
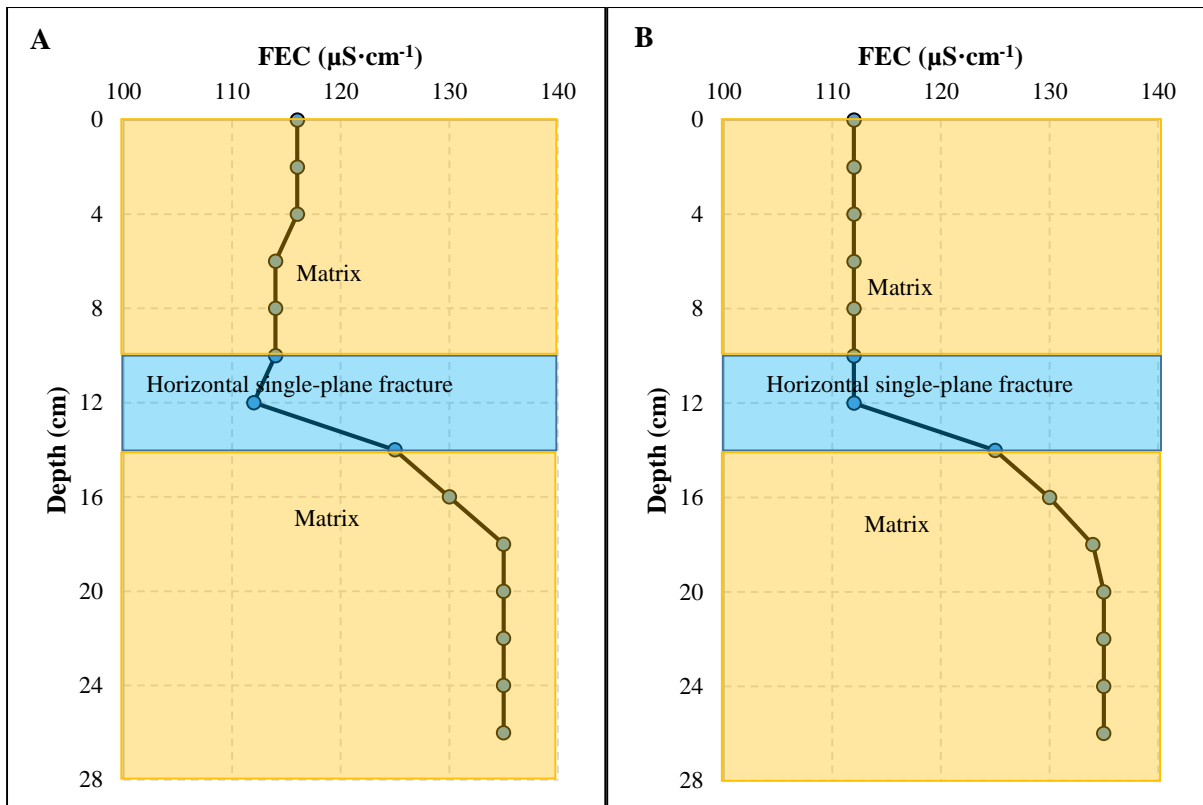


Figure 3-8 The variation in electrical conductivity of different soils. Sand naturally has the least FEC, silts have a medium FEC and clays have a high FEC (Adapted from Grisso *et al.*, 2009).

### 3.2.3.2 Background FEC Profile: Freshwater flow conditions

As freshwater started to flow through the system, FEC values started to change especially towards the top section (Figure 3-9 A-B), until the values at the top section were eventually similar to those observed at the fracture location (Figure 3-9 A-B). However, in the bottom section the FEC remained relatively high due to the limited flow (limited freshwater replenishment) in that region. Under freshwater flow conditions, the background FEC profile of the system ranged from 112 - 135  $\mu\text{S}\cdot\text{cm}^{-1}$ .



**Figure 3-9** FEC values obtained under freshwater flow conditions. The FEC of the system decreased as freshwater entered the system; a noticeable decrease was seen at the fracture position as well as at the water above the fracture, however the bottom matrix FEC values remained relatively high.

The incoming freshwater was lighter in density compared to the water already in the system, thus the freshwater not only moved laterally across the inflow zone (fracture) but some also migrated upwards due to the density contrast (Figure 3-10). This resulted in the dilution of water in the upper segment. Dilution continued until the FEC of the upper segment became similar to the FEC of the incoming freshwater. Since the freshwater cannot sink to the bottom, the FEC values of lower segment remained relatively high. This phenomenon can be related to that of seawater intrusion into aquifers; where less dense freshwater floats on top of denser saltwater (Figure 3-11).

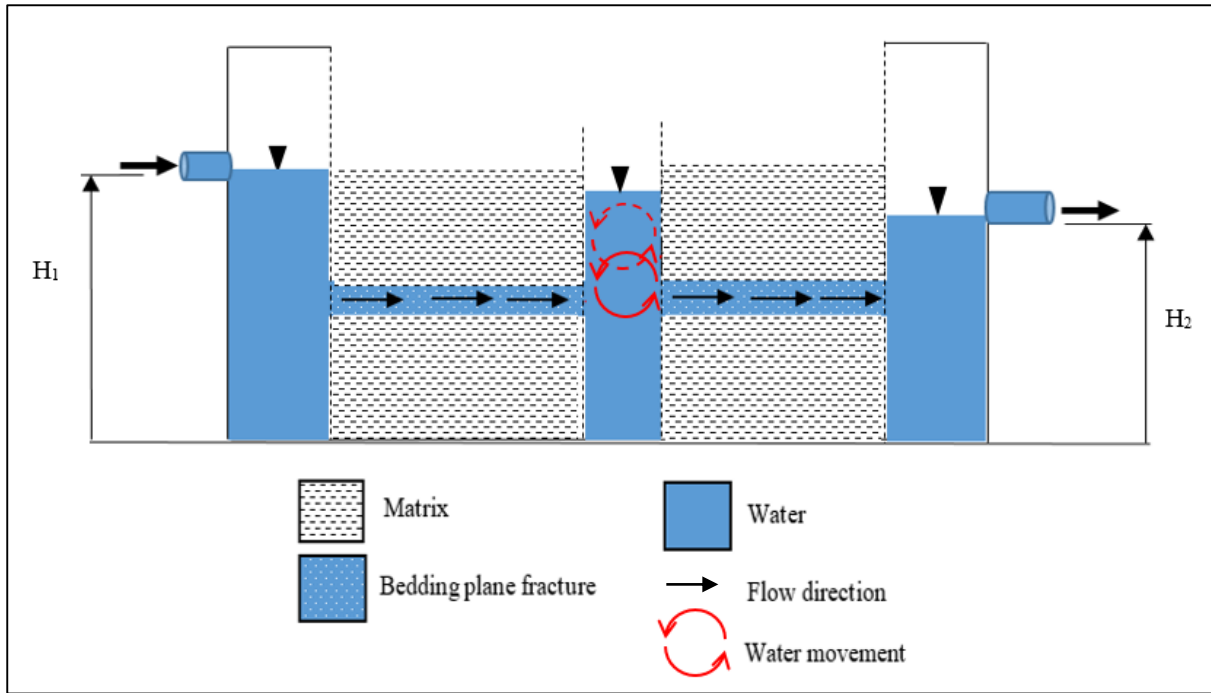


**Figure 3-10 Illustration of freshwater movement within the borehole. Since the freshwater which entered the borehole had a lower FEC compared to the water already in the system, the freshwater migrated upwards because it's lighter in density thus diluting the upper segment.**

The boundary between saltwater and freshwater is brackish with saltwater and freshwater mixing. This boundary can be likened to the transition zone of the observed FEC profiles which is indicated by an anomaly. This zone has been inferred to show the position of fractures in aquifers and is frequently targeted for the collection groundwater samples representative of aquifer water. However, the results of this study suggest that under freshwater flow conditions, groundwater samples representative of fracture water are more likely to be found from the fracture itself as well as the upper segment above the fracture position. The transition zone represents a mixture between fracture water and high TDS water from the lower matrix, thus does not exclusively represent fracture water.

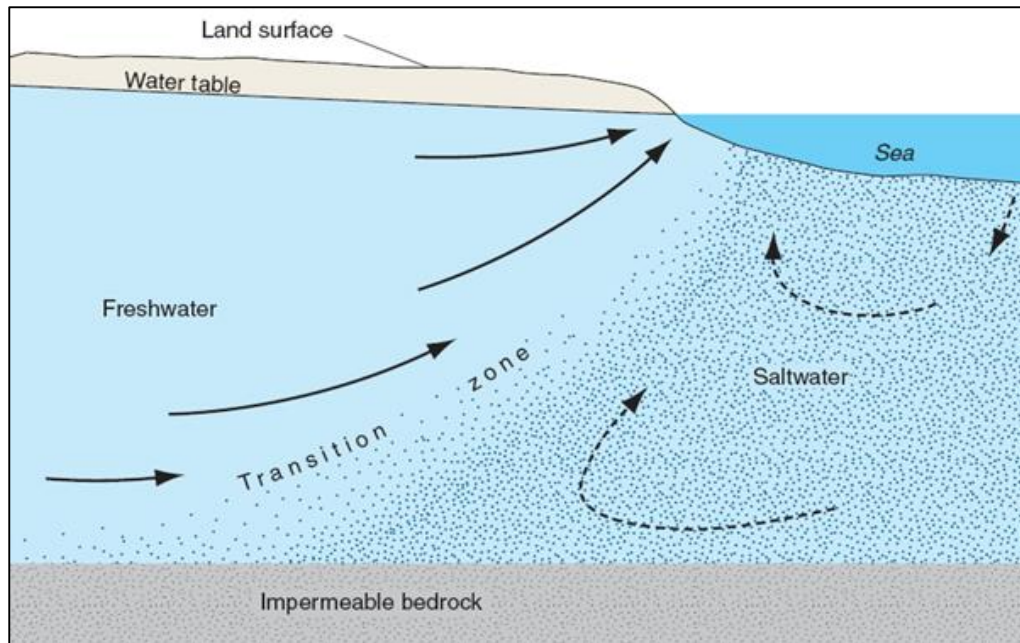


Figure 3-11 Seawater intrusion mixing concept; less dense freshwater floats on top of denser saltwater. The boundary (transition zone) between saltwater and freshwater is brackish with saltwater and freshwater mixing (Henry, 1964).

### 3.2.3.3 Plume arrival FEC profile

After injecting the tracer into the system, five mins later the plume had already reached the borehole, this led to a fairly unstable/inconsistent trend of the FEC profile (Figure 3-12). This behaviour is accounted for by the mixing which occurs between the freshwater already in the borehole and the incoming contaminated water. Additionally, the general effect of introducing the tracer into the system was that the denser solute migrated downwards instead of just moving laterally, which resulted in a significant increase in FEC values towards the bottom of the borehole.

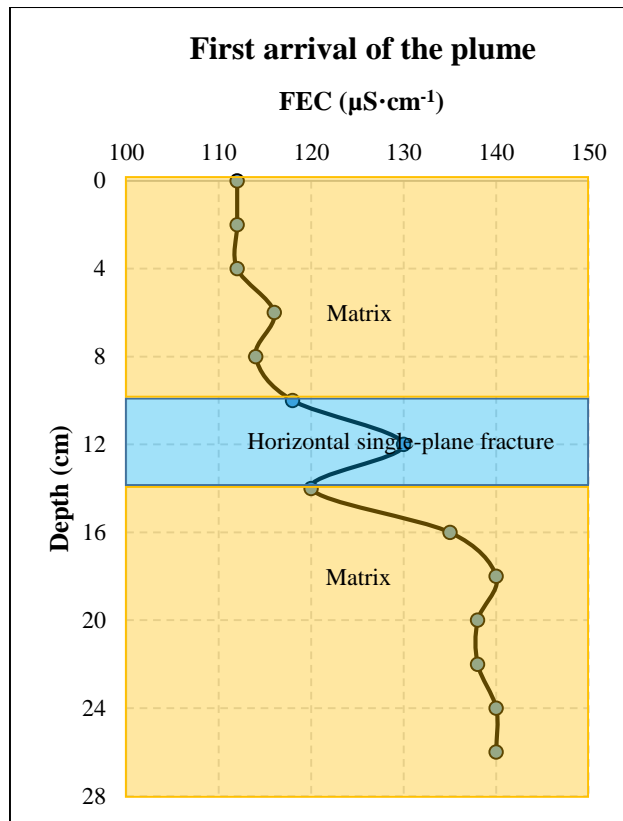


Figure 3-12 FEC profile five mins after injection of the saline water. A fairly unstable trend was observed as a result of the mixing which occurred between the fresh and contaminated water.

### 3.2.3.4 Plume peak FEC profile

The FEC profile associated with the arrival of the plume peak was obtained after 13 mins as informed by the observed peak breakthrough time acquired during the testing of the physical model. The profile showed a continuous increase in FEC throughout its entire length. However, due to density contrast (dense water sinks), the FEC values associated with the lower matrix were higher compared to the ones associated with the upper matrix. Since the fracture was the most transmissive formation of the system (thus acted as a preferential flow path to pollution), the highest FEC values were observed at its location (Figure 3-13). A maximum FEC value of  $2506 \mu\text{S}\cdot\text{cm}^{-1}$  was recorded at the fracture position. The same trend was also visible in a case study which was conducted in a contaminated borehole located in the Beaufort West town (Figure 3-14).

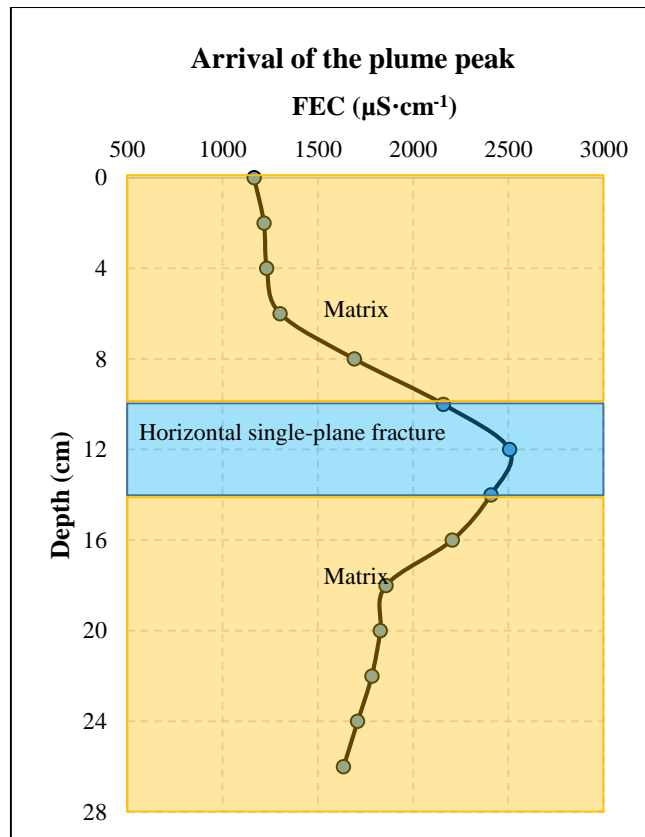


Figure 3-13 Arrival of the plume peak in the fracture was observed after 13 mins. Since the fracture was the most transmissive formation in the system the highest FEC values were observed at its location.

### 3.2.3.4.1 Case study example

Figure 3-14 shows an example of an FEC profile obtained from a contaminated borehole in a bedding plane fractured rock aquifer system located in the Beaufort West town, in the Western Cape Province, South Africa (Gomo, 2009). The study area falls under Beaufort Group of the main Karoo Supergroup. The Karoo Supergroup mainly constitute of sandstone, mudstone, shale and siltstone sedimentary rocks thus hosting typical horizontal bedding plane fractures. The aquifer was contaminated by dissolved light non-aqueous phase liquids (LNAPL) contaminants and a similar profile to that shown in Figure 3-13 was observed. The observed FEC anomaly between 22 - 24 mbgl was attributed to the fracture's transportation of biodegraded petroleum hydrocarbon contaminants. The process associated with the biodegradation of petroleum hydrocarbon contaminants has the potential to generate carbonic acid that can leach the formation's elements leading to elevated FEC values (Hiebert *et al.*, 1995).

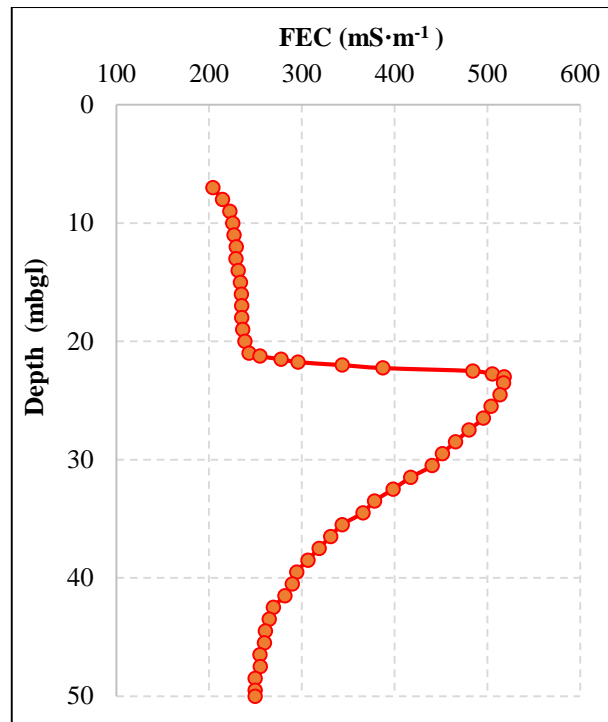


Figure 3-14 Profile obtained from a contaminated borehole in a fractured system located in Beaufort West town in South Africa (Gomo, 2009).

### 3.2.3.5 Residual plume FEC profile

After the contaminant plume passed the monitoring borehole and freshwater started entering the system, dilution took place and FEC values decreased (Figure 3-15). Most of the dilution was observed at the position of the fracture, this is because water enters the system and flows quicker at this position therefore constant replenishment of freshwater occurs. Also, due to the upward movement of the incoming freshwater (as indicated by Figure 3-10) the dilution which took place at the top (upper matrix) was more pronounced than the dilution at the bottom (lower matrix).



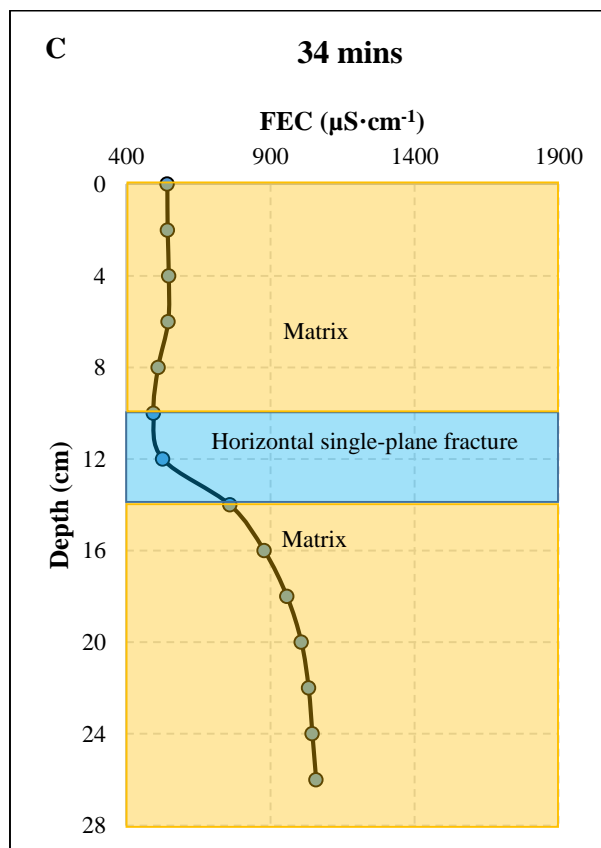
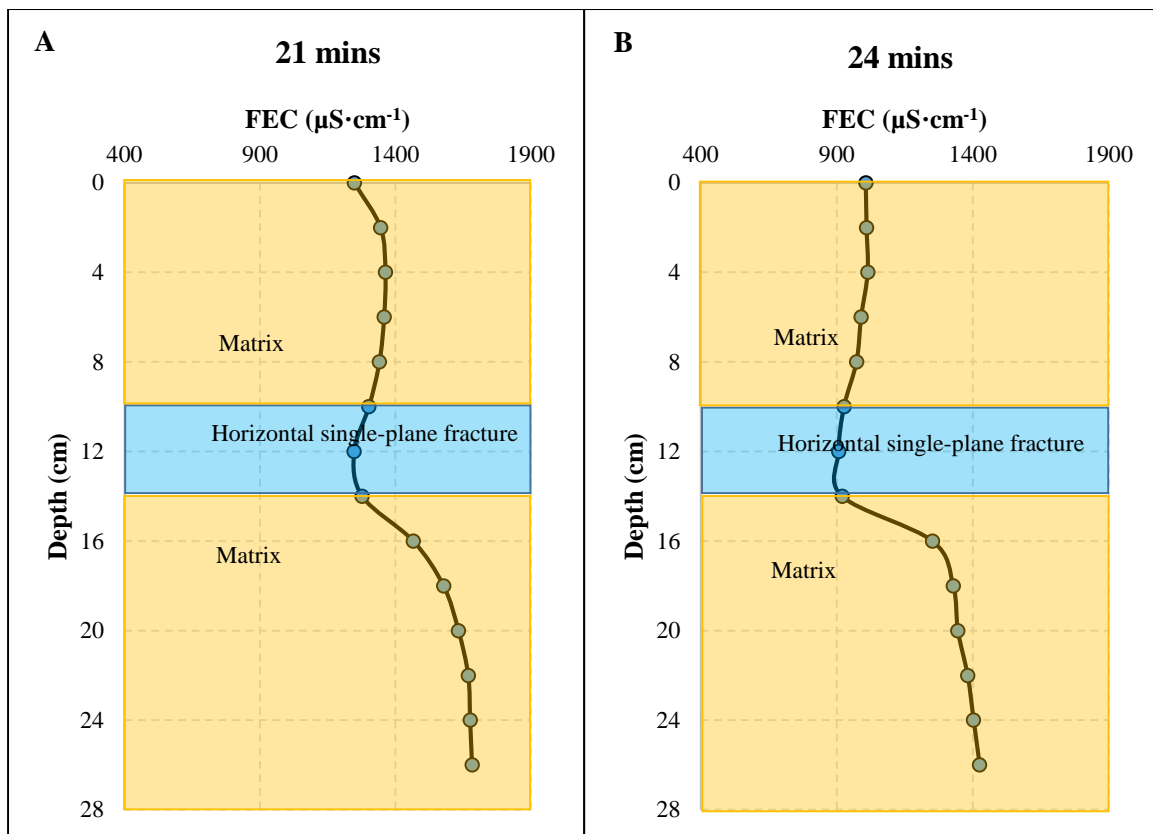


Figure 3-15 FEC profiles associated with the residual plume; once the contaminant plume passed the monitoring borehole, due to incoming freshwater the FEC values started to decrease.

### 3.2.3.6 Near background FEC profile

The system continued to dilute until the water above the fracture (upper segment) was similar to the fracture water in terms of its hydrochemistry characteristics. This suggests that one could actually sample from the top of the borehole and still get water that is representative of fracture-aquifer water (Figure 3-16). In certain zones along the borehole (i.e. the lower segment) the water did not dilute back to its initial (background) values; these zones were interpreted as low flow zones thus replenishment in these zones was limited. The FEC values at the top reached near background values after 2hrs 29mins, this was primarily due to the upward migration of freshwater in the borehole. It is important to note that given more time (for replenishment to take place) the FEC values throughout the entire profile would have gone back to the initially recorded background values.

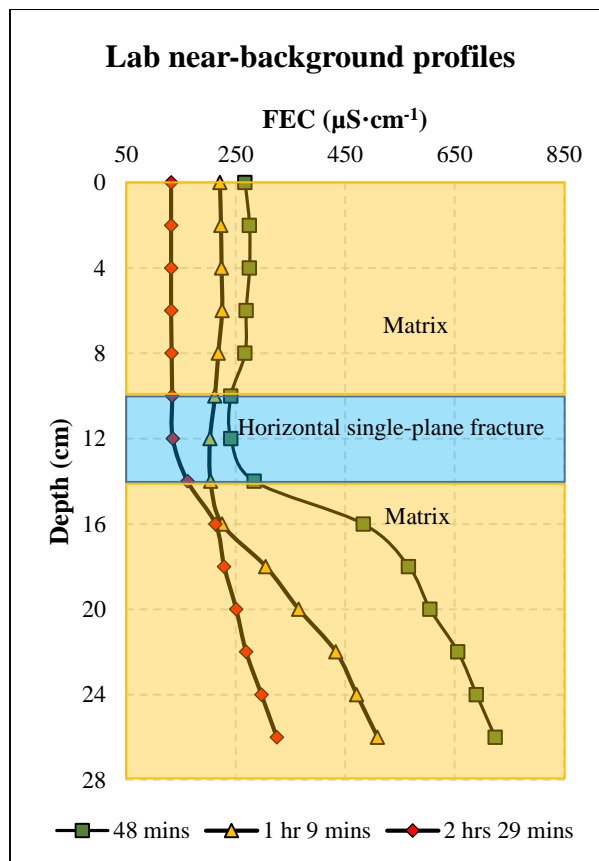


Figure 3-16 FEC profiles associated with near-background values. The freshwater which entered the borehole was less dense compared to the contaminated water already in the system, thus it migrated upwards and diluted the upper segment of the borehole. Diffusion was responsible for the dilution of the lower segment, and since it's a slower process the lower segment would take longer to reach background values.

The FEC values of the lower matrix took much longer to reach near-background values. This is because as a contaminant moves through a fractured rock system, it tends to diffuse from the flowing fracture water into the rock's stagnant pore water (in this case the matrix), this process retards the contaminant plume's progress through a fractured rock aquifer which leads to the prolonged increased FEC values observed at the bottom of the system (Figure 3-16). Although this could be beneficial in some cases, it is also challenging in other cases since it substantially increases the difficulty of purging contamination from the aquifer during remediation. According to Lever *et al.* (1985) matrix diffusion can lead to effective retardation and can reduce peak concentrations by three to four orders of magnitude, provided that the groundwater velocity is relatively small. The degree and hydro-geologic significance of the diffusion will depend upon the concentration gradient, the matrix diffusivity and porosity, the fracture spacing of the rock as well as the duration of exposure (Mutch, 1991).

Generally, the profiles (i.e. Figure 3-9, Figure 3-15 and Figure 3-16) show three distinct zones; the upper diluted zone (which is combined with the upper part of the fracture), the transition zone where an anomaly is observed and the higher FEC zone located at the bottom. This is illustrated in Figure 3-17.

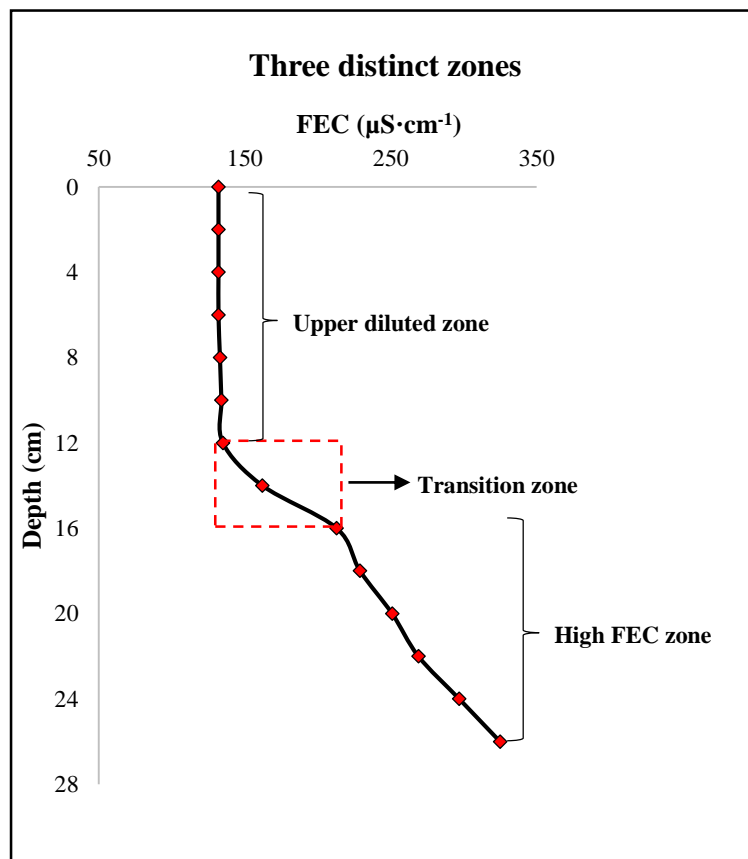


Figure 3-17 Profiles showing three distinct zones; the upper diluted zone; the transition zone and the high FEC zone.

## **4 FIELD EXPERIMENT**

A forced-gradient tracer breakthrough test was conducted at the University of the Free State Campus Test Site which consists of a horizontal bedding-plane fracture. The main objective of this test was to compare the differences and similarities between results obtained in the laboratory with ones from the field. The forced-gradient was achieved through pumping at a low rate and was only applied to reduce the time it would take for the tracer to travel through the system. Three boreholes were used; UO3 as the injection borehole, CH2 as a monitoring borehole and BH as the pumping borehole.

### **4.1 Description of the test site**

The Campus Test Site is a relatively uncontaminated horizontal bedding-plane fractured rock aquifer system, which is used for academic studies and research by the Institute for Groundwater Studies (IGS). It is located at the University of the Free State in Bloemfontein, South Africa. It covers an area of approximately 35 000 m<sup>2</sup> and has been used as a facility to conduct various geophysical, hydraulic, and chemical transport investigations in fractured sedimentary rocks (i.e. Botha *et al.*, 1997; Botha *et al.*, 1998; van Wyk *et al.*, 2000; Chiang and Riemann, 2000; Riemann, 2002). The site has 52 boreholes which have been drilled, some which have been displayed in Figure 4-1. Only the boreholes highlighted in blue were used in this study.

The site is partially situated on a basal outcrop of the Spitskop Sandstone but is mainly on the underlying Campus Sandstone. Outcrops of the mudstones that overlie the Campus Sandstone are surficial and are covered by brown soil and clay. The drainage is described as medium to good and the soil structure as stable (Botha *et al.*, 1998). In general, the landscape is easily accessible.

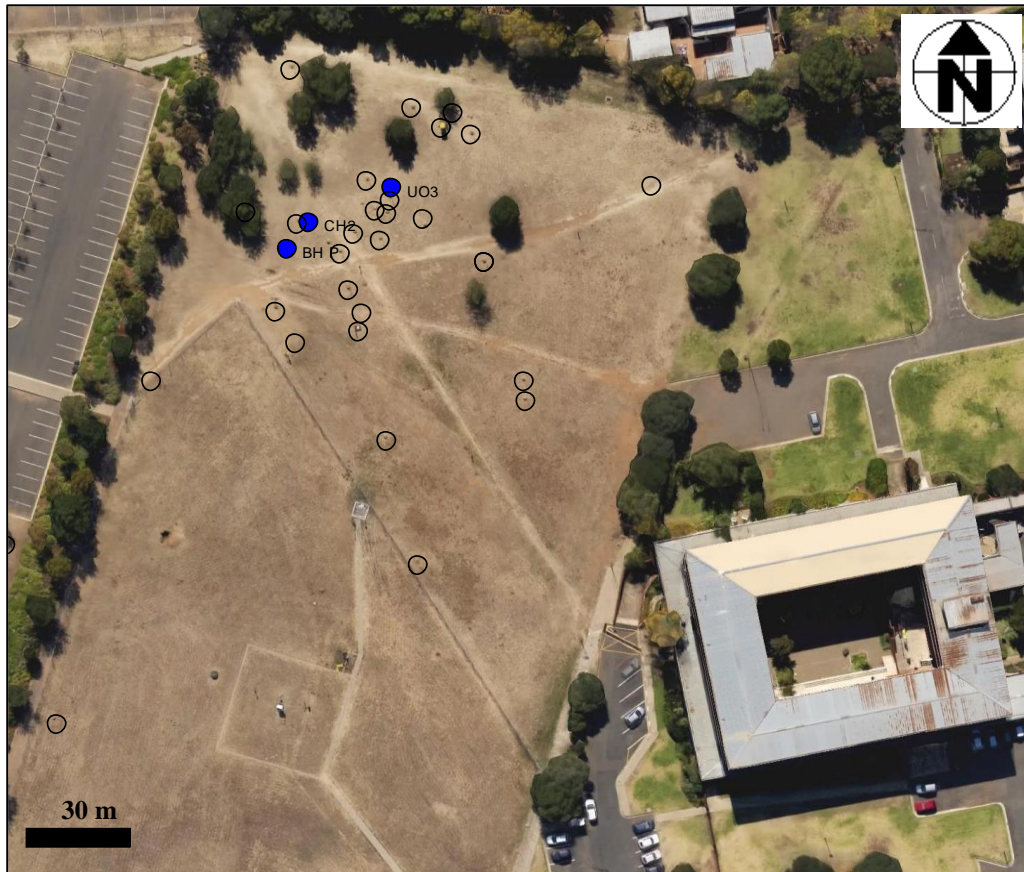


Figure 4-1 Plan view of some of the boreholes at the Campus Test Site, the blue boreholes represent ones used for this study; BH, CH2 and UO3.

#### 4.1.1 Geology and Hydrogeology

According to van Tonder and Vermeulen (2005) the Campus Test Site is underlain by a series of Karoo sandstones, mudstones and shales which were deposited under fluvial environments of the Adelaide Subgroup of the Karoo Supergroup. The Karoo Supergroup characteristically consists of sandstone, shale, siltstone and mudstone. The local geology and hydrogeological conditions of the Campus Test Site has been well documented in previous studies (Botha *et al.*, 1998; van Wyk *et al.*, 2000; Chiang and Riemann, 2000; Riemann 2002). From the borehole logs obtained from boreholes UO3 (injection borehole) and CH2 (monitoring borehole) it is evident that mudstone, siltstone, shale and sandstone formations exist on the site (Figure 4-2).

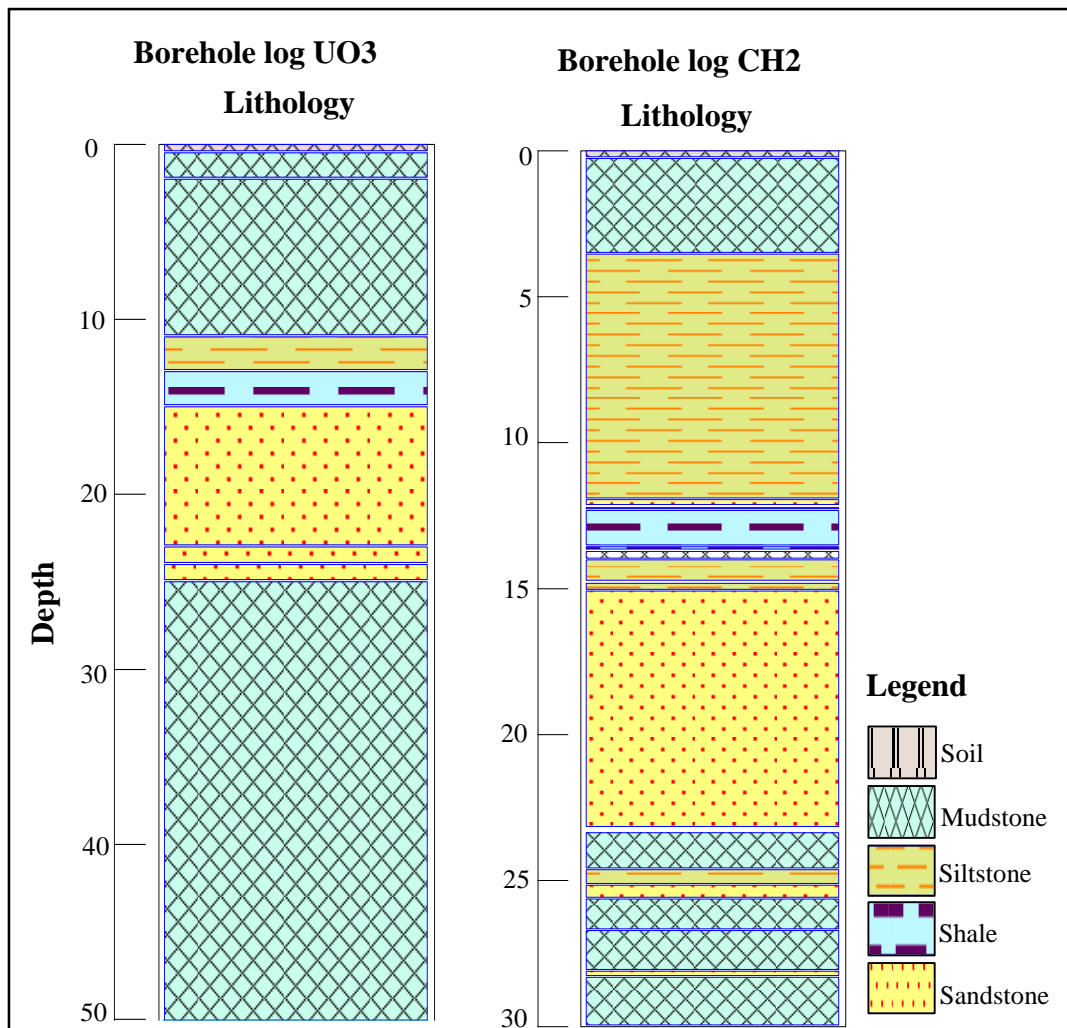


Figure 4-2 Lithological logs of the injection borehole (UO3) and the monitoring borehole (CH2).

According to Botha *et al.* (1998) there are three aquifers present on the Campus Test Site (Figure 4-3). The top aquifer has been distinguished as a phreatic aquifer that is situated in the upper mudstone layers on the site. The top mudstone is unconfined and extends roughly to a depth of 14 meters (m) below land surface, and is characterised by a very low yield. This aquifer is separated from the middle and main aquifer by a layer of carbonaceous shale which is 0, 5 m to 4 m thick. The second and main aquifer occurs in a sandstone layer that is 8 m to 10 m thick. The high transmissivity of this unit is attributed to the horizontal fracture at 21.2 m. This fracture at the Campus Test Site closely resembles the horizontal single-plane fractured aquifer kind of system. Although the fracture occurs at a depth of 21.2 m in the schematic diagram below (Figure 4-3), it is not consistently located at this depth throughout the entire site. At certain locations within the site, it is positioned higher or lower (i.e. at the monitoring borehole CH2, it is located at a depth of 18.4 -20.4 m). The third aquifer occurs in the mudstone

layers that underlie the sandstone unit and is more than 100 m thick. The mudstone unit at the bottom of the sequence also has a low yield similar to the unconfined aquifer.

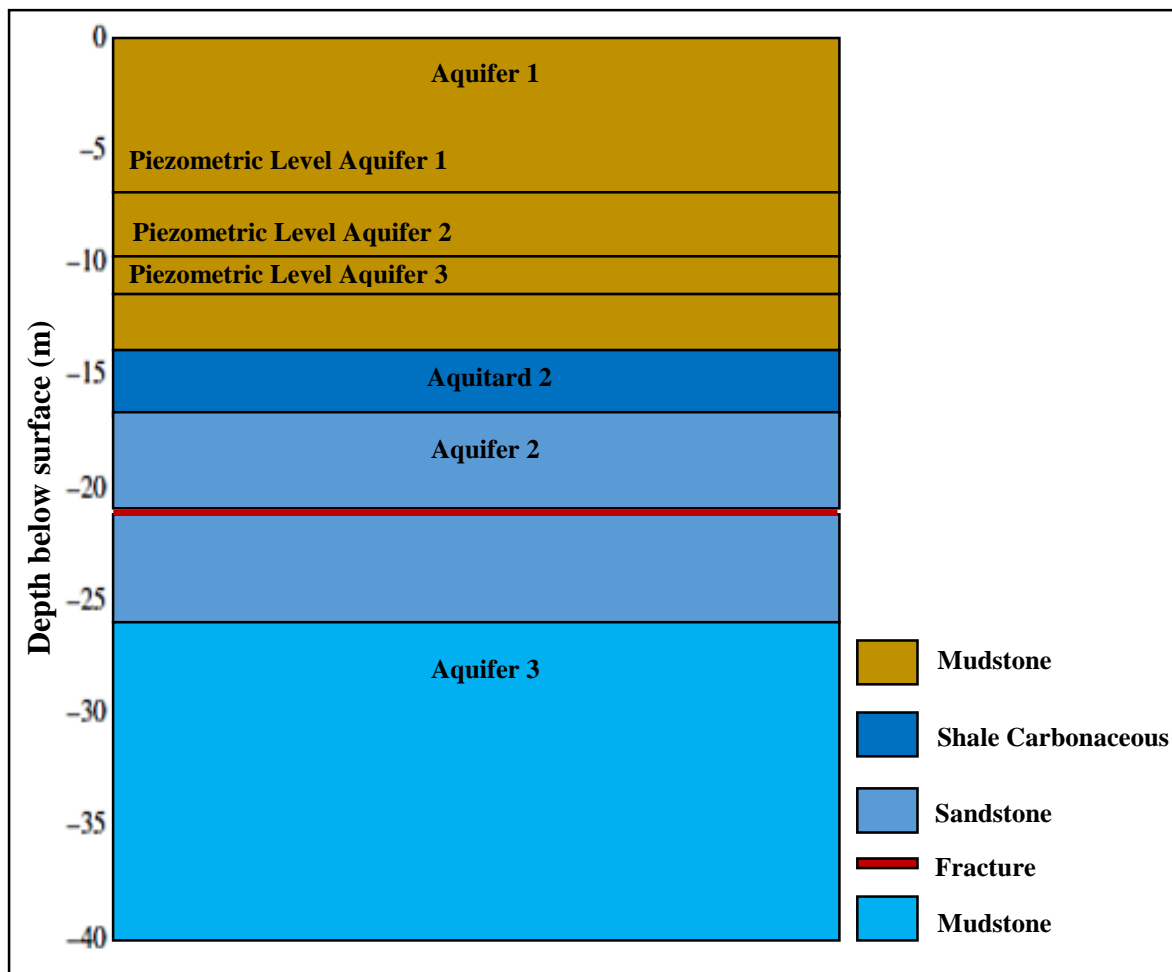


Figure 4-3 Schematic diagram of the different geological formations and aquifers present on the Campus Test Site (Modified from Botha and Cloot, 2004).

## 4.1.2 Hydraulic and mass transport parameters

### 4.1.2.1 Darcy’s velocity and effective porosity

A series of tracer tests (point dilution, radial convergent) have been carried out on the Campus Test Site to provide information on the travel times of water in the aquifer as well as to determine aquifer parameters, the geometry of fractures and the role of fractures of different apertures in contaminant migration (i.e. Xu *et al.*, 1997; Botha *et al.*, 1998; Pacome, 2010). From these tests it was determined that the natural groundwater velocity in a sedimentary rock can be as high as 27 m/day, the calculated effective porosity at the scale of the fracture zone has been determined to be 30 % (van Wyk, 1998).

### 4.1.2.2 Hydraulic conductivity

The Campus Test Site is mainly characterised by parallel bedding plane fractures, situated along the contours of a sandstone unit. From the geological outcrops the existence of extensional fractures (mode I) and shearing fractures (mode II) has been observed by Riemann (2002). Double packer tests conducted on the site by Botha *et al.* (1998) yielded average horizontal conductivity values (Figure 4-4) for more prominent formations. An average value of 23.79 m/day was determined for the mode I fracture.

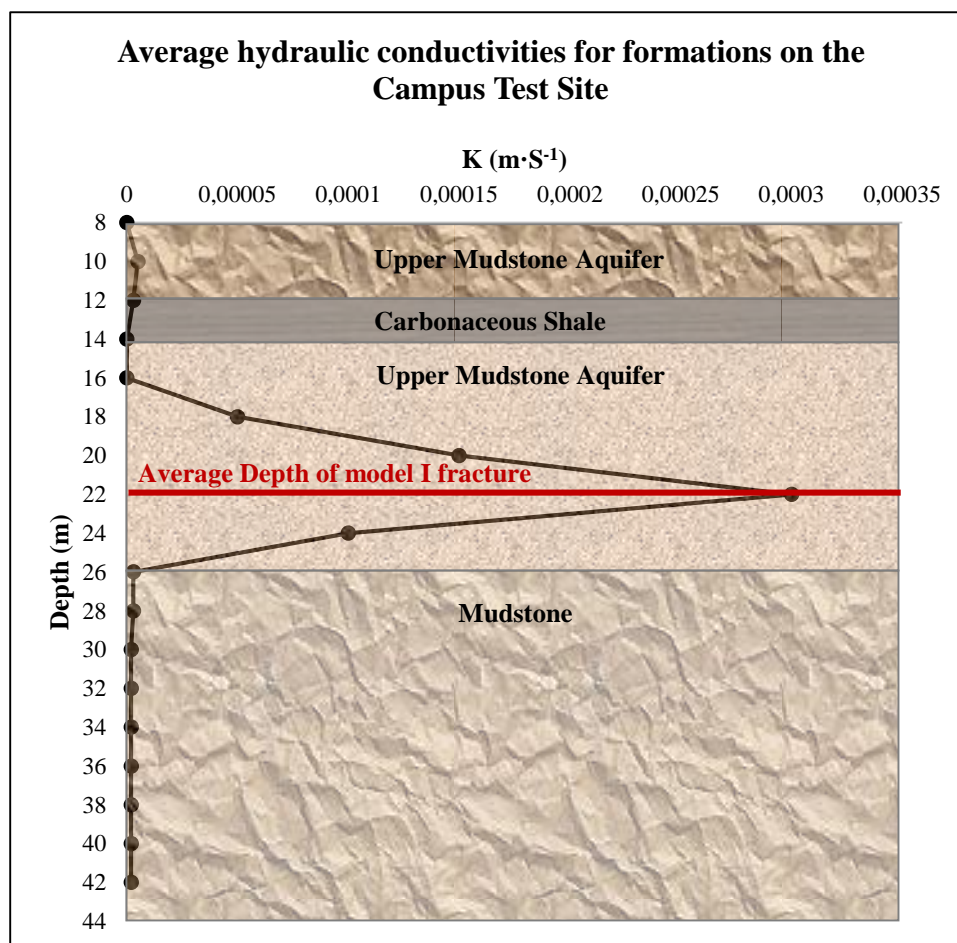


Figure 4-4 Average hydraulic conductivities (K) for the more prominent formations on the Campus Test Site as determined from double packer tests (Modified from Pacome, 2010).

## 4.2 Methods and materials

Three boreholes were used; UO3 as the injection borehole (located 20 m from the pumping borehole), CH2 as a monitoring borehole (located 15 m from the pumping borehole) and BH as the pumped borehole. The hydraulic heads of the injection and monitoring boreholes were



at 14.69 and 15.10 mbgl respectively, and 16.29 mbgl at the pumping borehole. Sodium chloride (NaCl) was the only tracer used in this experiment.

BH was pumped at a constant rate of 2  $\ell$ /s. Pumping continued until a constant hydraulic head (pseudo-state condition) was established between the injection borehole and the monitoring borehole. Thereafter, the FEC of groundwater in the borehole was slightly increased by introducing NaCl into the injection borehole (UO3) using an injection sock which was tied to a rope (Figure 4-5). The sock was slowly lowered down and up the borehole so that a significant change in the salinity of the groundwater throughout the borehole was created.



**Figure 4-5** Salt was introduced into the injection borehole using an injection sock which was tied to a rope. The sock was slowly lowered down and up the borehole so that significant change in the salinity of the groundwater throughout the borehole was created.

Immediately after the sock was pulled out of the borehole column, the concentration of the tracer was monitored (at the monitoring borehole) in terms of its FEC using the TLC probe. A pull-up profiling protocol was used to profile the borehole at a fairly constant rate. The probe is designed so that water flows over the sensor while it is being lowered and was set to take readings every 5 seconds. The head and FEC values were both recorded by the sensor simultaneously, this eliminates data mismatch. The logger depth data was corrected to depth below casing by adding the static water level to the recorded depth.

Theoretically, if groundwater flow is the only factor controlling the tracer movement, more dilution would be expected at sections of higher groundwater flow. As a result, the FEC values would be more pronounced (once the tracer was added) at areas with higher groundwater velocity, thus fracture positions or sections of higher hydraulic transmissivities would be easily identified.

The experiment continued for six hours until the tracer concentration was depleted and enough data was accumulated for interpretation and comparison purposes.

## **4.3 Results and discussion**

### **4.3.1 Background FEC profile**

Before the start of the test FEC profiles in the monitoring borehole (CH2) were obtained and the results are graphically illustrated in Figure 4-6A. The general trend observed is higher FEC values towards the bottom compared to the upper section. It is worth noting that the pre-test FEC values at the upper section of CH2 ranged from 862-871  $\mu\text{S}\cdot\text{cm}^{-1}$  and the FEC values towards the bottom ranged from 986-1011  $\mu\text{S}\cdot\text{cm}^{-1}$ .

According to borehole logs (Figure 4-2) the increase in FEC towards the bottom can be accounted for by the low permeability mudstone situated in that section; due to its low hydraulic conductivity, the replenishment is limited. However, at a depth of approximately 15-22 mbgl lower FEC values can be seen, this is because of the presence of a more permeable sandstone layer; due to its fairly high flow velocity and hydraulic conductivity, it allows for a constant inflow of freshwater into the system thus replenishment of the section.

In general, the shape of the background profile observed in the field was closely comparable to the one observed in the laboratory experiment (Figure 4-6B); low FEC at the top and higher FEC at the bottom.

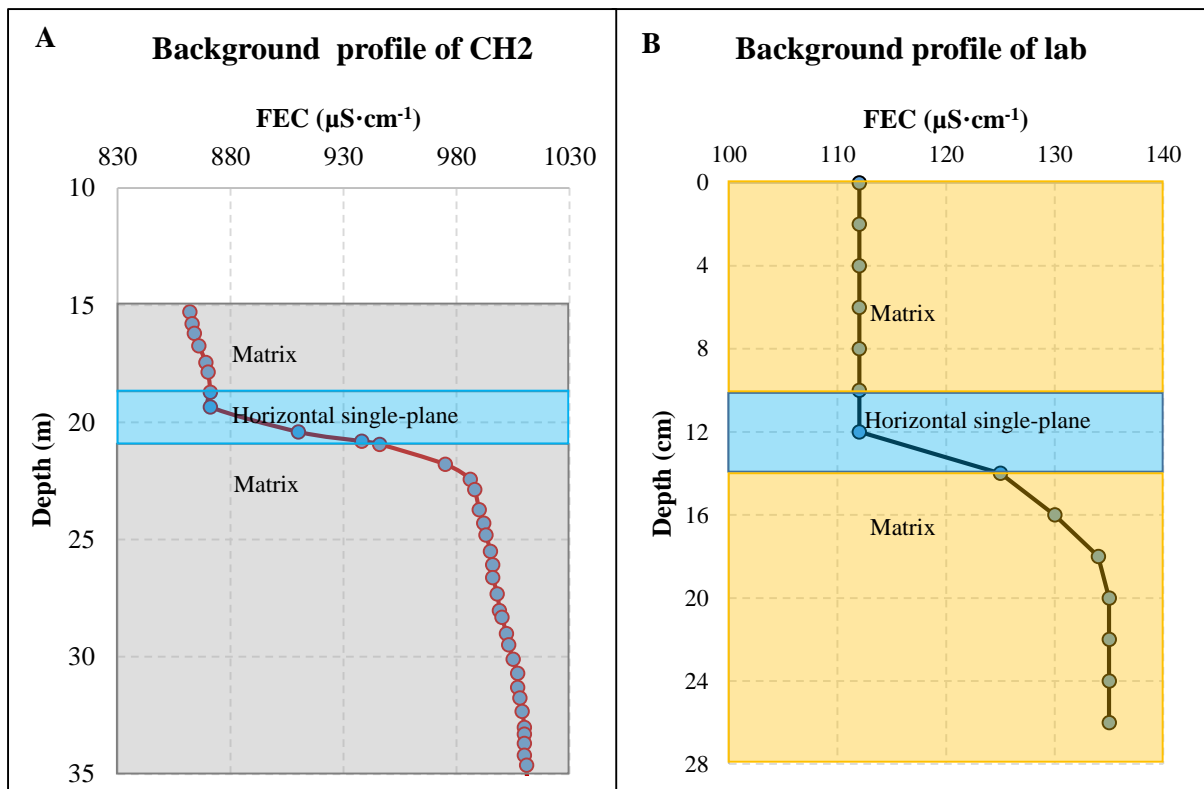


Figure 4-6 The background FEC profile of (A) the field monitoring borehole (CH2) and (B) the laboratory monitoring borehole before the tracer was injected. A general trend of low FEC values at the top and higher FEC values at the bottom were observed.

#### 4.3.2 First arrival of plume FEC profile

As salt was introduced into the system, 19 mins later the plume had already reached the permeable segment (fracture) of the CH2 borehole and FEC values slightly increased from  $840 \mu\text{S}\cdot\text{cm}^{-1}$  to  $887 \mu\text{S}\cdot\text{cm}^{-1}$  (Figure 4-7A). However unlike in the laboratory experiment (Figure 4-7B), there were no visible changes in the shape of the profile; the background profile of CH2 and its first arrival profile looked relatively similar. This was due to the large scale in the field; even-though the FEC had slightly increased, the change was not substantial enough to cause a noticeable disturbance to the system hence the trend remained the same.

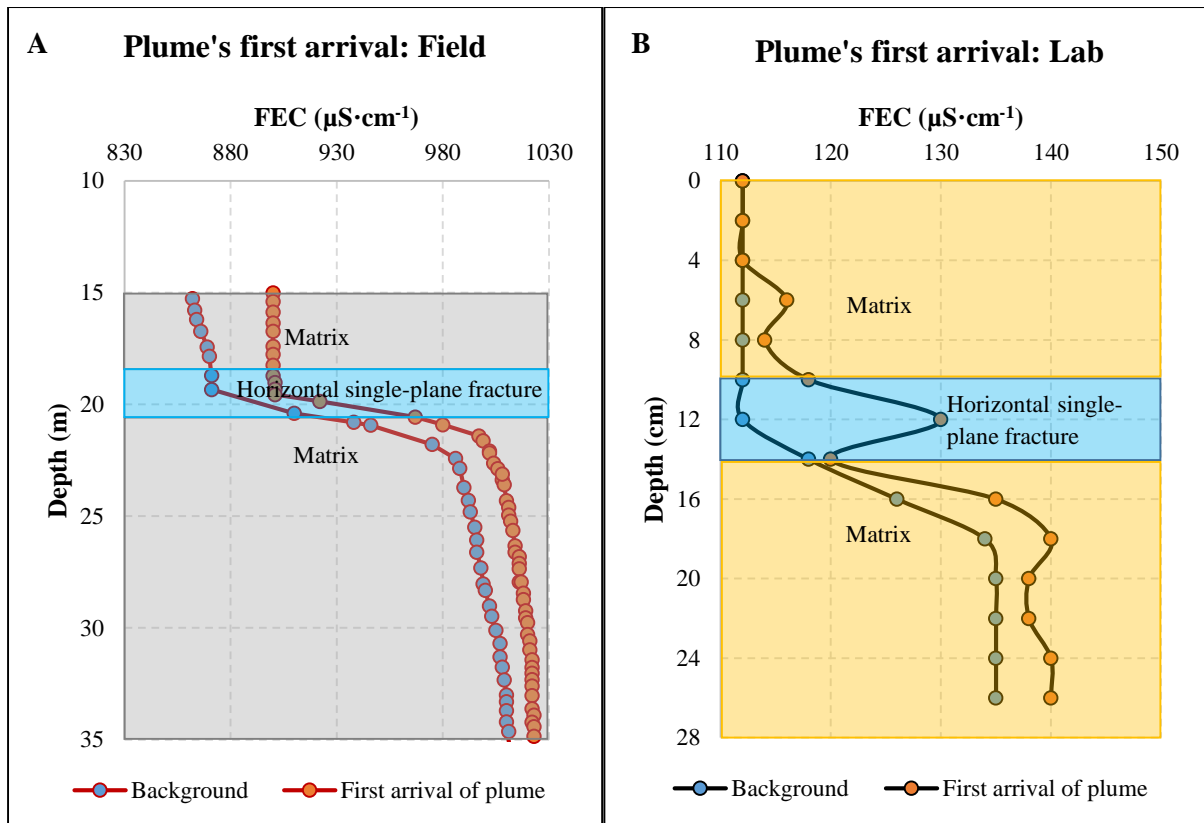


Figure 4-7 The background profile versus the plume's first arrival profile (A) in the field and (B) in the laboratory.

### 4.3.3 Plume peak FEC profile

A continuous increase in FEC was observed throughout the system until a maximum value of  $1616 \mu\text{S}\cdot\text{cm}^{-1}$  was reached at the fracture position 54 mins later (Figure 4-8A). Generally, a contaminant is most likely to travel through a path of less resistance (preferential flow path), therefore, a more pronounced anomaly was observed at the fracture position due to its high transmissivity and groundwater velocity. A similar trend was observed in the laboratory results (Figure 4-8B) as well as in a fractured rock aquifer system contaminated with LNAPLs (Figure 3-14); whereby the most elevated FEC values were observed at the position of the fracture. However, unlike in the laboratory experiment the density effects (whereby saline contaminated water sinks to the bottom) in the field were significantly reduced but not entirely eliminated. This reduction could be due to various factors such as:

- The use of an injection sock; which did not abruptly alter the salinity of the water in the borehole but instead slowly changed it as it was lowered down and up.
- Due to pumping, ample volume of freshwater was able to enter the system at a faster rate which quickly diluted the tracer and reduced its density.

- The scale factor; the field experiment was conducted on a larger scale relative to the laboratory experiment.

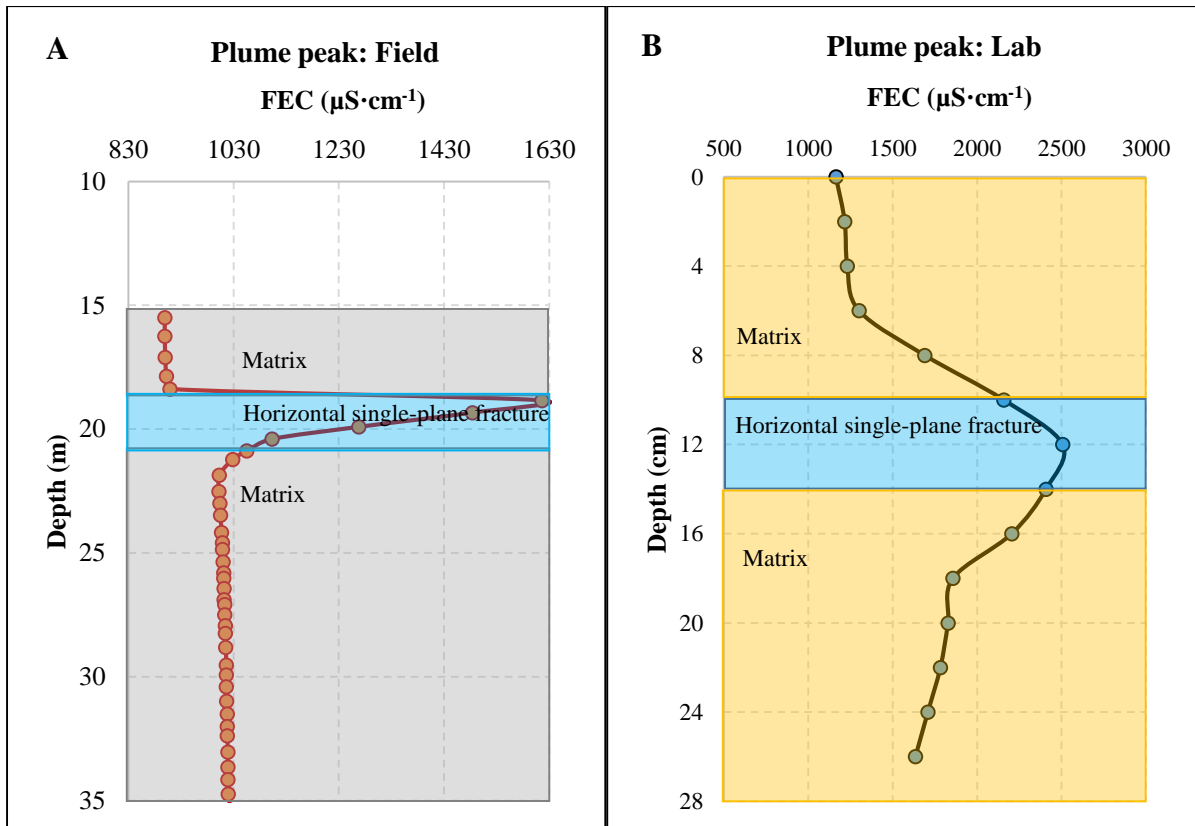


Figure 4-8 FEC profile associated with the plume peak in (A) the field monitoring borehole and (B) the laboratory monitoring borehole. The most elevated FEC values were observed at the position of the fracture where the highest transmissivity and groundwater velocity is.

#### 4.3.4 Residual plume FEC profile

Once the plume peak passed through the monitoring borehole dilution took place, 1 hr 57mins later (Figure 4-9A) the FEC of the upper segment of the borehole slightly decreased from  $899 \mu\text{S}\cdot\text{cm}^{-1}$  to  $888 \mu\text{S}\cdot\text{cm}^{-1}$ , the fracture position decreased from  $1616 \mu\text{S}\cdot\text{cm}^{-1}$  to  $1104 \mu\text{S}\cdot\text{cm}^{-1}$  and the bottom segment of the borehole decreased from  $1020 \mu\text{S}\cdot\text{cm}^{-1}$  to  $1010 \mu\text{S}\cdot\text{cm}^{-1}$ . It is evident that most of the dilution occurred at the fracture position this is due to constant freshwater replenishment taking place.

It can be observed in Figure 4-9A and B that dilution was more drastic in the laboratory experiment than it was in the field (even-though there was pumping involved in the field). This is because the laboratory experiment was conducted on a much smaller scale relative to the field scale; therefore, the contaminant was able to migrate through the system much quicker

with less constraints. This in turn limited the diffusion of the contaminant into the matrix which reduced the residence time of the plume in the system.

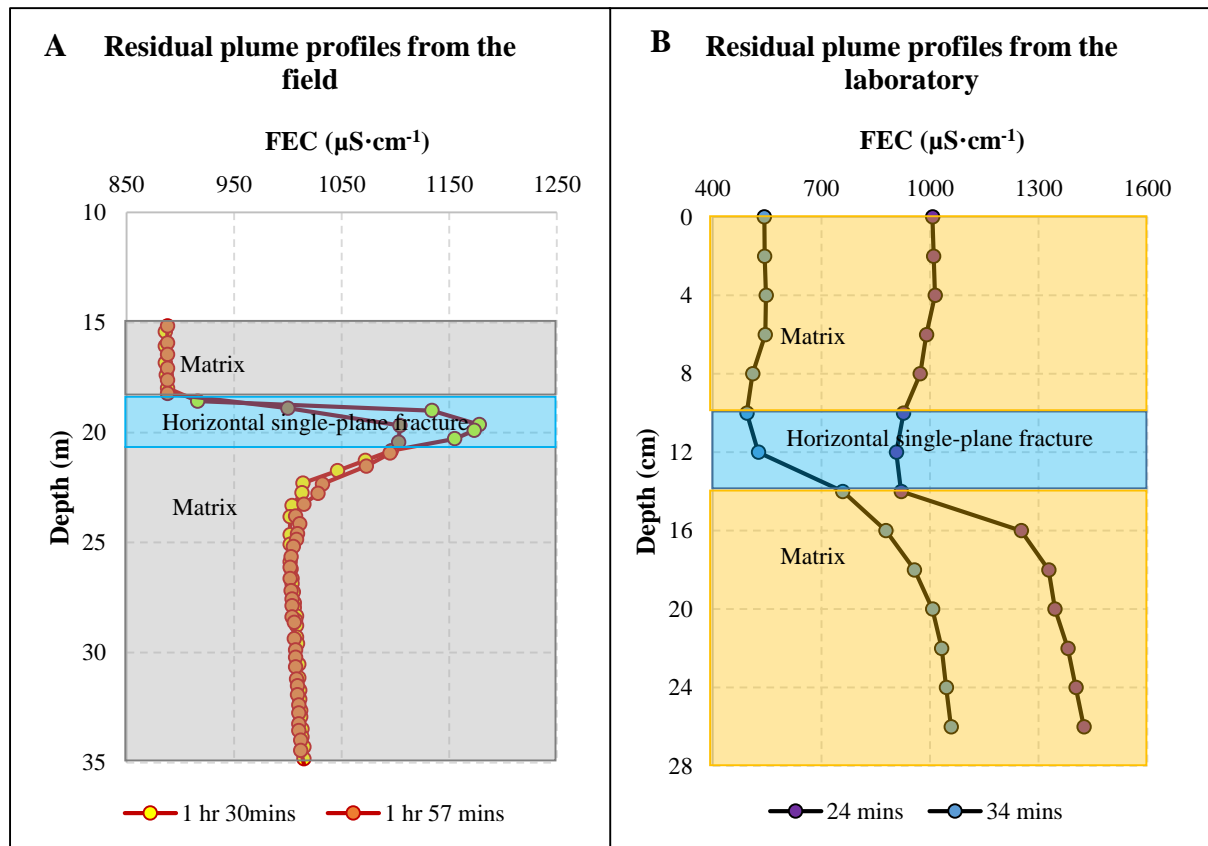


Figure 4-9 Profiles associated with the residual plume in (A) the field and (B) the laboratory. Dilution in the laboratory was more rapid than it was in the field. This can be accounted for by the scale factor; the laboratory experiment was conducted on a much smaller scale compared to the field test.

#### 4.3.5 Near background FEC profile

Continuous dilution took place until FEC reached near-background values in the range of 868-881  $\mu\text{S}\cdot\text{cm}^{-1}$  in the upper segment, 1009-1037  $\mu\text{S}\cdot\text{cm}^{-1}$  in the fracture position and 1003-1014  $\mu\text{S}\cdot\text{cm}^{-1}$  in the bottom segment (Figure 4-10). Contrary to the laboratory experiment, dilution at the upper and bottom segment took place at the same rate. The dilution of the upper segment can still be accounted by the upward movement of the incoming freshwater. The pumping in the field may have increased the rate of diffusion in the bottom segment.

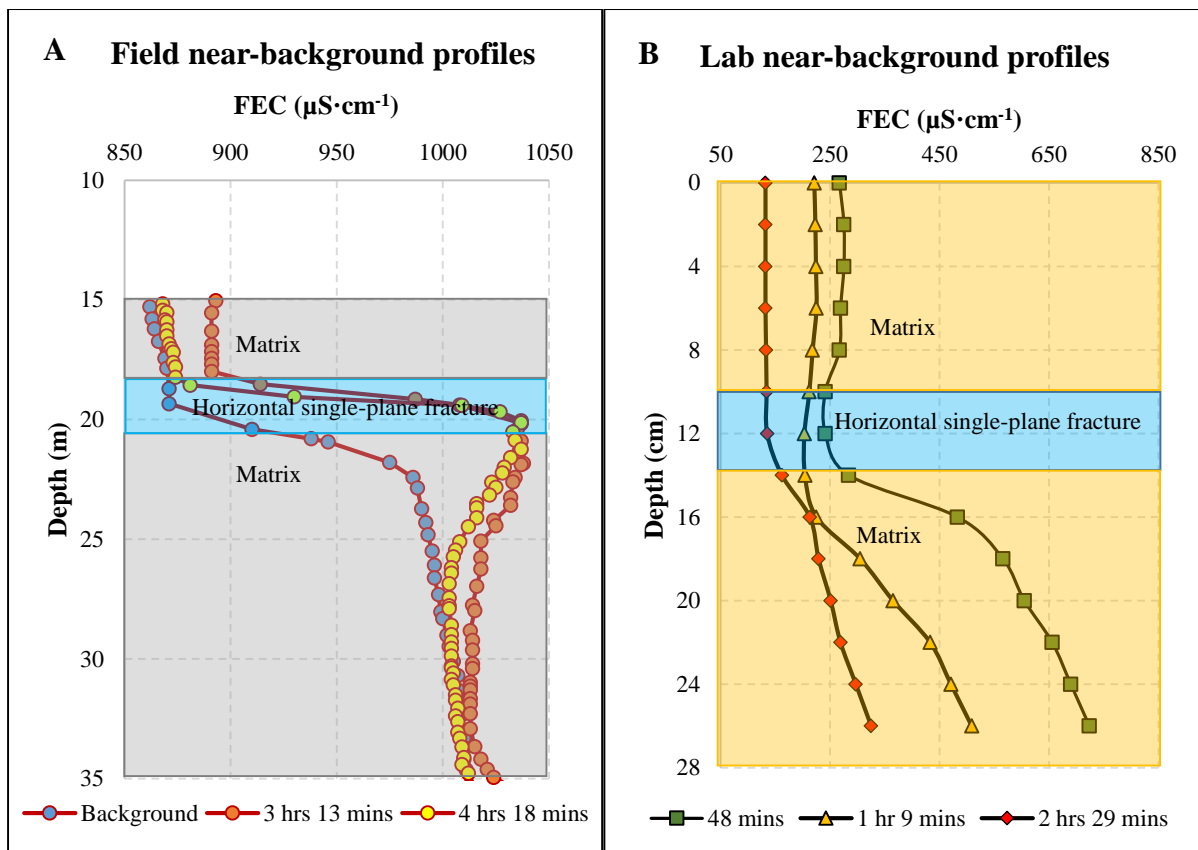


Figure 4-10 FEC profiles associated with near-background values (A) in the field and (B) in the laboratory. Due to the large scale, the system took much longer to reach near background values in the field compared to the laboratory.

The shape of profiles which were obtained at the field was comparable to those observed in the laboratory experiment thus increasing the confidence of the accuracy and relevance of the laboratory results.

#### **4.4 Study limitations**

- The coarse grained sand which was used to simulate the fracture may not behave exactly like an actual fracture (opening) in terms of its hydraulic characteristics (i.e. porosity and/or transmissivity), this may to some extent have influenced the results.
- A bigger aquifer (physical model) could have been built to facilitate the recording of more measurements and also to eliminate variations encountered due to the scale factor.
- Additionally, the field test was conducted under forced gradient conditions, perhaps slightly different results would have been observed if the tracer migrated on its own under natural conditions. However, the general shape of the profile isn't expected to change because most of the transportation of the saline plume would still occur in the fracture.

In general, based on the aims of this study, it is unlikely that the abovementioned limitations had a significant influence on the results observed.



## 5 CONCLUSIONS AND RECOMMENDATIONS

### 5.1 Conclusions

Laboratory tests were conducted with the use of a physical model to investigate the evolution of fluid electrical conductivity (FEC) profiles associated with a contaminant plume, in a horizontal single-plane fractured rock aquifer system. To achieve this two groundwater flow and transport conditions were simulated; one with freshwater flow and the other with saline contaminated water. Generally, two distinct profiles associated with a contaminant plume in a borehole drilled in a horizontal single-plane fractured rock aquifer were identified and can be conceptualised as follows:

#### 5.1.1 Conceptual background profile

The conceptual background profile was observed under natural conditions (freshwater flow), this profile was also similar to the residual plume profile as well as the near-background profile (in terms of shape). Essentially, within this profile three distinct segments (zones) were noted; the upper segment, transition zone and the lower segment (Figure 5-1).

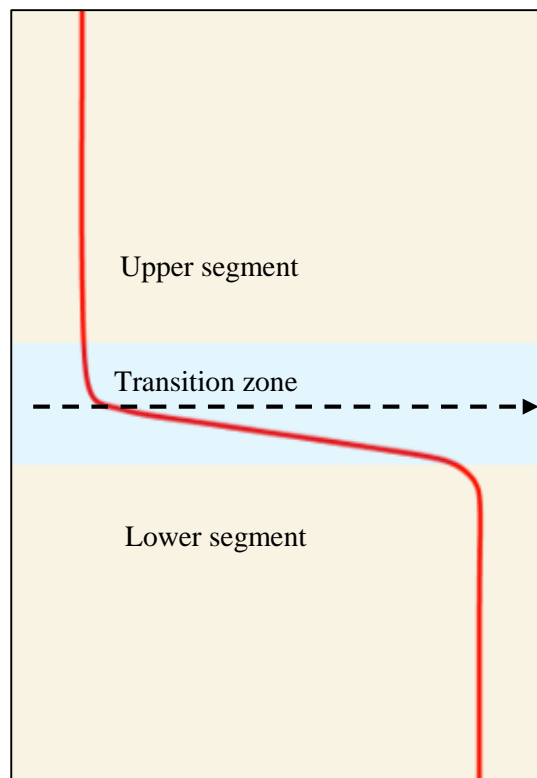


**Figure 5-1** The background profile, which was observed under natural conditions (freshwater flow). This profile was also similar to the residual plume profile as well as the near-background profile in terms of shape. The arrow in the centre indicates the maximum velocity within the fracture.

The fracture was the most transmissive formation in the system; therefore, it facilitated the inflow of freshwater into the system thus resulting in low FEC values. Although the upper and lower segment were equally low in permeability, had the same transmissivity and were therefore expected to have the same FEC values, however, this was not the case. Instead the upper matrix had lower FEC values, this was because it diluted faster due to the density contrasts between the incoming lighter freshwater (which entered through the fracture) and the denser stale water already in the system. Since the incoming freshwater had a lower density relative to the water already in the system, it migrated upwards thereby diluting the upper segment of the aquifer. Dilution continued until the water above the fracture (the upper matrix) was similar to the water of the aquifer in terms of quality and hydrochemistry.

Within the horizontal single-plane aquifer system, the highest velocity was found at the centre of the fracture aperture (as indicated by the arrow in Figure 5-1); the velocity decreased towards the edges of the fracture as illustrated by Raven *et al.* (1988) in Figure 2-8. Therefore, most of the replenishment took place at the centre of the fracture and since the inflowing freshwater was lighter in density compared to the water already present in the system, it ultimately migrated towards the top of the system. As a result, the upper part of the fracture was composed of representative aquifer water, whereas the lower part was the transition zone. The transition zone is the boundary where the inflowing fresh fracture water comes into contact with the high FEC lower matrix water. The lower matrix diluted at a much slower rate because diffusion was the only factor decontaminating it, and this is usually a slow process.

### **5.1.2 Conceptual elevated FEC profile**

The second conceptual profile is associated with elevated FEC values; it was observed when a contaminant associated with increased FEC values reached the monitoring borehole (Figure 5-2). Its anomaly would be more or less pronounced (at the fracture position) depending on the stage of the contaminant plume within the system. Since the fracture was the most transmissive part of the system it acted as a preferential flow path which allowed the contaminant to move through it at a faster rate hence the observed FEC anomaly. The peak values were observed at the centre of the fracture aperture where the highest velocity was.

As freshwater continued to flow through the system, the contaminant started to dilute, most of the dilution was observed at the high inflow zone. Because the bottom layer was less permeable it limited replenishment, and due to diffusion (of the solute into the matrix) some of the

contaminant was retained by this layer, thus higher FEC values remained at the bottom section of the system for a prolonged period of time.

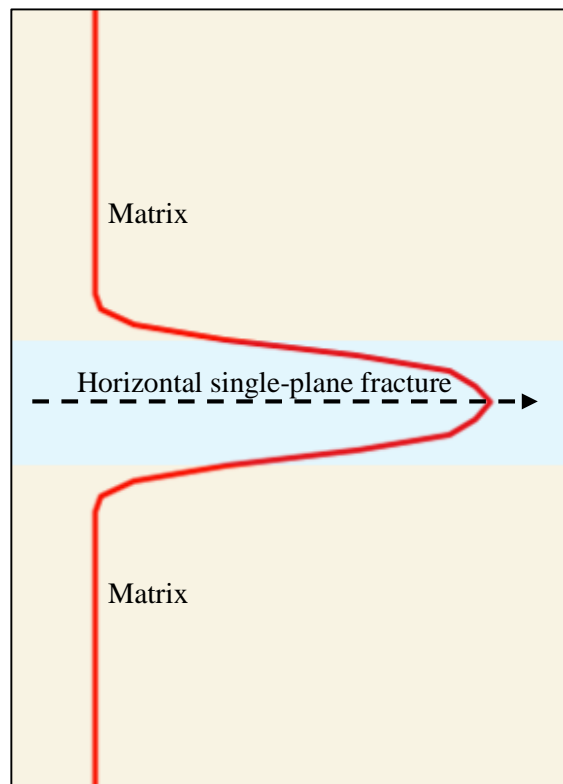


**Figure 5-2 Profile associated with elevated FEC values; observed when a contaminant plume reached the monitoring borehole. The highest FEC values were observed at the centre of the fracture aperture where the highest velocity is present (as indicated by the arrow).**

These profiles were observed under a controlled laboratory environment and were also verified in the field. The profiles which were obtained in the field were comparable to those observed in the laboratory experiment thus increasing the confidence of the accuracy of the laboratory results.

The insight gained from this study can assist in guiding the interpretation of FEC profiles. It can also assist users in identifying the stage of the contaminant plume within the aquifer system at the time of FEC profiling. Furthermore, the location of groundwater flow zones is of great importance as it assists in obtaining representative aquifer water, this study offers a recommendation (discussed below) which can be applied on the pursuit of acquiring representative aquifer water based on FEC data.

## 5.2 Recommendations

The following recommendations are made based on the findings of the study:

The background profile illustrated that in a horizontal single-plane fractured aquifer system, continuous dilution takes place until water above the fracture (upper segment) is similar to the incoming aquifer water in terms of quality and hydro-chemistry. This observation suggests that one could actually sample from the top of the fracture position (upper segment) and still get groundwater water which is representative of the fracture water (Figure 5-3). Although it is mostly common to sample at the transition zone, it is clear that the water at that position does not entirely represent aquifer water but is instead a mixture between aquifer water and water from the matrix. Therefore, it would be more ideal to sample towards the top of the fracture.

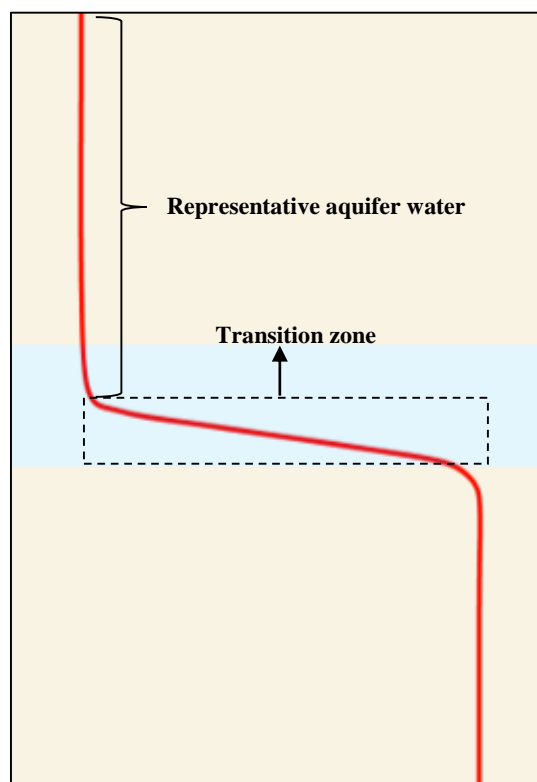


**Figure 5-3** The water towards the top of the fracture is more representative of aquifer water, whereas the water at the transition zone is a mixture of aquifer and lower- matrix water.

Insight gained from controlled laboratory investigations of FEC profiles can provide guidelines for the interpretation of data collected from field tests. Additionally, while monitoring, it is recommended that FEC profiling is performed before sampling. Samples usually provide data only from the sampled depth intervals and results may only be obtained after laboratory

analysis, whereas FEC profiling offers continuous readings which can be analysed in real time at the test site. This can be used to guide completion or testing procedures.

Future studies can consider using an actual fracture opening when conducting laboratory experiments such as the one conducted in this study for better results. Furthermore, similar experiments can be conducted on other aquifer types in order to improve the general understanding across different aquifer systems.

## 6 REFERENCES

- Abelin, H., Birgersson, L., Moreno, L., Widen, H., Agren, T. and Neretnieks, I. (1991).** A large-scale flow and tracer experiment in granite 2. Results and interpretation. *Water Resources Research*, 27(12), pp. 3019–3135.
- Akoachere, R.A. and Van Tonder, T. (2009).** Two new methods for the determination of hydraulic fracture apertures in fractured-rock aquifers. Revised version. *Water SA*, 35 (3). ISSN 0378-4738. ISSN 1816-7950: *Water SA* (on-line). Available on website <http://www.wrc.org.za>. [Accessed on 11 Jan 2017].
- Bäumle, R. (2003).** Geohydraulic Characterisation of Fractured Rock Flow Regimes. Regional Studies in Granite (Lindau, Black Forest, Germany) and Dolomite (Tsumeb Aquifers, Northern Namibia). PhD Thesis, Department of Applied Geology, Karlsruhe, Germany.
- Bear, J. (1972).** Dynamics of Fluids in Porous Media. New York, London (Elsevier), pp. 764.
- Bear, J. and Cheng, A.H.D. (2010).** Modelling Groundwater Flow and Contaminant Transport. In: *Theory and Applications of Transport in Porous Media*, vol. 23. Springer, pp. 834.
- Bear, J., Tsang, C.F. and de Marsily, G. (Eds.) (1993).** Flow and Contaminant Transport in Fractured Rock. New York (Academic Press Inc.), pp. 560.
- Beauheim, R.L., Meigs, L.C. and Davies, P.B. (1997).** Rationale for the H-19 and H-11 tracer tests at the WIPP site, Field tracer experiments: role in the prediction of radionuclide migration, synthesis and proceedings of an NEA/EC GEOTRAP workshop, Cologne, Germany, 28-30 August 1996, OECD-NEA, Paris, France, 107-118. ISBN 92-64-16013-2.
- Beauheim, R.L. and Pedler, W.H. (2009).** Technical Report: Fluid Electrical Conductivity Logging in Borehole DGR-1. Doc ID: TR-07-14. DGR Site Characterization Document Inter-Engineering Project 06-219.
- Becker, M. W., Reimus, P. W. and Vilks, P. (1999).** Transport and attenuation of carboxylatemoified-latex microspheres in fractured rock laboratory and field tracer tests. *Ground Water* 37 (3), pp. 387-395.
- Becker, M. W. and Shapiro, A. M. (2000).** Tracer transport in fractured crystalline rock: Evidence of nondiffusive breakthrough tailing. *Water Resour. Res.* 36 (7), pp. 1677-1686.

**Beven, K. and Young, P. (2013).** A guide to good practice in modelling semantics for authors and referees. *Water Resources Research* 49, pp. 5092-5098.

**Botha, J. F., Verwey, J.P., Van der Voort, I., Vivier, J.J.P., Buys, J., Colliston, W.P. and Looch, J.C. (1997).** Karoo aquifers: Their geology, geometry and physical properties. Report to the Water Research Commission of South Africa.

**Botha, J. F., Verwey, J. P., Van der Voort, I., Vivier, J. J. P., Colliston, W. P. and Looch, J. C. (1998).** Karoo Aquifers. Their Geology, Geometry and Physical Behaviour. Water Research Commission. South Africa.

**Broding, R.A. (1982).** Volumetric scanning well logging. *The Log Analyst* 23, pp. 14 – 19.

**Darcy, H.P.G. (1856).** Determination of the Laws of Water Flow through Sand, the Public Fountains of the City of Dijon, Appendix D- Filtration, section 2 of Appendix D on Natural Filtration. Translated from French by Patricia Bobeck. Kendall/ Hunt Publishing Company, Iowa, pp. 455-459.

**De Marsily, G. (1986).** Quantitative hydrology: groundwater hydrology for engineers. Ed. 2. Academic Press. Paris, France.

**Doughty, C. and Tsang, C.-F. (2000).** BORE II – A Code to Compute Dynamic Wellbore Electrical Conductivity Logs with Multiple Inflow/Outflow Points Including the Effects of Horizontal Flow Across the Well. Rep. LBL-46833, Lawrence Berkeley National Laboratory, Berkeley, CA.

**Doughty, C and Tsang, C.-F. (2002).** Inflow and outflow signatures in flowing wellbore electrical- conductivity logs, Rep. LBNL- 51468. Berkeley, CA: Lawrence Berkeley National Laboratory.

**Doughty, C., Tsang, C.-F. (2004).** (revised version of 2000) BORE II—A code to compute dynamic wellbore electrical conductivity logs with multiple inflow/outflow points including the effects of horizontal flow across the well, Rep. LBNL-46833, Lawrence Berkeley\ National Laboratory, Berkeley, CA.

**Doughty, C. and C.-F. Tsang. (2005).** Signatures in flowing fluid electric conductivity logs. *Journal of Hydrology.*, 310, pp. 157 – 180, doi:10.1016/j.jhydrol. 2004.12.003

**Doughty, C., Takeuchi, S., Amano, K., Shimo, M. and Tsang, C.-F. (2005).** Application of multi-rate flowing fluid electric conductivity profiling method to well DH-2, Tono Site, Japan. *Water Resources Research.*, 41, W10401, doi: 10.1029/2004WR003708.

**Doughty, C., Tsang, C.-F., Hatanaka, K., Yabuuchi, S. and Kurikami, H. (2008).** Application of direct-fitting, mass integral, and multirate methods to analysis of flowing fluid electric conductivity logs from Horonobe, Japan, *Water Resources Research.*, 44, W08403, doi: 10.1029/2007WR006441.

**Doveton, J. H. and Prenskey, S. E. (1992).** Geological Applications of Wireline Logs: A Synopsis of Developments and Trends. *The Log Analyst*, 33 (3), pp. 286-30.

**Drost, W., Klotz, D., Koch A., Moser H., Neumaier F. and Rauert W. (1968).** Point dilution methods of investigating groundwater flow by means of radioisotopes. *Water Resour, Resear.*, 4 (1), pp.125–146.

**Elsler, P.L., Huppert, P., Wylie, A.W. (1971).** Logging of copper in simulated boreholes by gamma spectroscopy: 1. Activation of copper with fast neutrons, *Geo-exploration* 9, pp.181–194.

**Evans, D.G. (1995).** Inverting fluid conductivity logs for fracture inflow parameters. *Water Resource Research* 31 (12), pp. 2905–2915.

**Fujinawa, K., Iba, T., Fujihara, Y and Watanabe, T. (2009).** Modelling interaction of fluid and salt in an aquifer/ lagoon system. *Groundwater* 47 (1), pp.35-48.

**Gebrekrstos, R.A. (2007).** Site Characterisation Methodologies for DNAPLs in Fractured South African Aquifers. PhD thesis. Institute for Groundwater Studies. Faculty of Natural and Agricultural Sciences. University of the Free State, Bloemfontein, South Africa.

**Gehrels, H. and Gieske. A.S.M. (2003).** Aquifer Dynamics. In: Ian Simmers. *Understanding Water in a Dry Environment: Hydrological Processes in Arid and Semi-arid zones.* IAH Int Contrib Hydrogeol 23. A.A. Balkema, Tokyo, ISBN 90 5809 618 1. pp. 211-250.

**Gelhar, L.W. (1986).** Stochastic subsurface hydrology from theory to applications. *Water Resources Res.*, 22 (9), pp. 135-145.



**Gochioco, L.M., Magill, C. and Marks, F. (2002).** The Borehole Camera: An Investigative Geophysical Tool Applied to Engineering, Environmental, and Mining Challenges. – *The Leading Edge* 21(5), pp. 474 – 477.

**Gomo, M. (2009).** Site Characterisation of LNAPL – Contaminated Fractured - Rock Aquifer. MSc thesis. Institute for Groundwater Studies. Faculty of Natural and Agricultural Sciences. University of the Free State, Bloemfontein, South Africa.

**Gomo, M. (2011).** A groundwater-surface water interaction study of an alluvial channel aquifer. Ph.D. thesis. Institute for Groundwater Studies. Faculty of Natural and Agricultural Sciences. University of the Free State, Bloemfontein, South Africa.

**Gomo, M. and Vermeulen, D. (2015).** An investigative comparison of purging and non-purging groundwater sampling methods in Karoo aquifer monitoring wells. *Journal of African Earth Sciences*, 103, pp. 81–88.

**Gomo, M., Vermeulen, D. and Lourens P. (2017).** Groundwater Sampling: Flow-Through Bailer Passive Method Versus Conventional Purge Method. *Natural Resources Research*. doi:10.1007/s11053-017-9332-9.

**Grau, J.A., Schweitzer, J.S. and Hertzog, R.C. (1990).** Statistical uncertainties of elemental concentrations extracted from neutron-induced gamma-ray measurements, *IEEE Trans. Nucl. Sci.* 37, pp. 2175–2178.

**Grisak, G.E. and Pickens, J.F. (1980).** Solute transport through fractured media. 1. The effect of matrix diffusion. *Water Resour. Res.* 16 (4), pp. 719-730.

**Haggerty, R. S., McKenna, S.A. and Meigs, L.C. (2000).** Late time behaviour of tracer test breakthrough curves. 36 (12), pp. 3467-3479. doi: 10.1029/2000WR900214.

**Hale, F.V and Tsang, C.-F. (1988).** A Code to Compute Borehole Conductivity Profiles from Multiple Feed Points. Rep. LBL-24928, Lawrence Berkeley Laboratory, Berkeley, CA.

**Hiebert, F.K., Bennet, P.C., Folk, R.L. and Pope, S.R. (1995).** Enhanced mineral alteration by petroleum biodegradation in a freshwater aquifer in Microbial process for bioremediation, (Eds), Balle Press. Columbus, pp. 297 – 308.

**IAEA (International Atomic Energy Agency) (1999).** Nuclear Geophysics and its Applications. International Atomic Energy Agency, Technical Reports Series, 393, Vienna.

**Illman, W.A., Berg, S.J. and Yeh, T.-C.J. (2012).** Comparison of approaches for predicting solute transport: Sandbox experiment. *Groundwater* 50 (3), pp.421-431.

**Jardine, P.M., Sanford, W. E., Gwo, J.P., Reedy, O.C., Hicks, D.S., Riggs, J.S. and Bailey, W.B. (1999).** Quantifying diffusive mass transfer in fractured shale bedrock, *Water Resour. Res.* 35 (7). pp. 2015-2030.

**Jorgensen, D.G. and Petricola M., (1995).** Research Borehole-Geophysical Logging in Determining Geohydrologic Properties. – *Ground Water* 33(4). pp. 589 – 596.

**Keys, W.S., (1996).** A practical guide to borehole Geophysics in Environmental Investigations. – Lewis Publishers, Boca Raton, Florida.

**Kobr, M., Mares, S. and Paillet, F. (2005).** Geophysical Well Logging – Borehole Geophysics for Hydrogeological Studies: Principles and Applications. – In: Rubin Y & Hubbard SS (Eds.): *Hydrogeophysics*. Amsterdam. Springer, pp. 291 – 331.

**Krammer, K. (1997).** Geophysikalische Bohrlochmessungen bei der Erkundung von Deponiestandorten. – In: Beblo M (Ed.): *Umweltgeophysik*. Ernst, Berlin.

**Kruseman, G. P. and de Ridder, N.A. (1994).** Analysis and Evaluation of Pumping Test Data. Second Edition. International Institute for Land Reclamation and Improvement. Wageningen. The Netherlands.

**Kurikami, H., Takeuchi, R. and Yabuuchi, S. (2008).** Scale effects and heterogeneity of hydraulic conductivity of sedimentary rocks at Horonobe URL site. *Physics and Chemistry of the Earth* 33(2008) S37-S44.

**Le Borgne, T., Bour, O., Riley, M.S., Gouze, P., Perzard, P.A., Belghoul, A., Lods, G., Le Provost, R., Greswell, R.B., Ellis, P.A., Isakov. E. and Last. B.J. (2007).** Comparison of alternative methodologies for identifying and characterising preferential flow paths in heterogeneous aquifers. *J. Hydrol.* 345, pp. 134-148. doi: 10.1016/j.jhydrol.2007.07.007.

**Lee, C. and Farmer, I. (1993).** Fluid flow in discontinuous rocks. Chapman and Hall. pp. 169.

**Lever, D.A., Bradbury, M.H. and Hemingway, S.J. (1985).** The effect of dead-end porosity on rock-matrix diffusion. *J. Hydrol.* 80, pp. 45-76.

- Maloszewski, P. and Zuber, A. (1985).** On the theory of tracer experiments in fissured rocks with a porous matrix. *J. Hydrol.* 79. pp. 333-358.
- Maloszewski, P. and Zuber, A. (1990).** Mathematical modelling of tracer behaviour in short-term experiments in fissured rocks. *Water Resour. Res.* 26 (7), pp. 1517-1528.
- Maloszewski, P., Herrmann, A. and Zuber, A. (1999).** Interpretation of tracer test performed in fractured rock of the Lange Bramke basin, Germany. *J Hydrol.* 7, pp. 209-218.
- Mamer, E.A. and Lowry, C.S. (2013).** Locating and quantifying spatially distributed groundwater/ surface water interactions using temperature signals with paired fiber-optic cables. *Water Resources Research* (49), pp. 1-11.
- Mares, S., Zboril, A. and Kelly, W.E. (1994).** Logging for the Determination of Aquifer Hydraulic Properties. – *The Log Analyst* 35(6), pp. 28 – 36.
- Maute, R.E. (1992).** Electrical logging: State-of-the-art. – *The Log Analyst* 33(3), pp. 206 – 227.
- McNeely, R. N., Neimanis V. P. and Dwyer., L. (1979).** *Water Quality Sourcebook (A Guide to Water Quality Parameters)*. Inland waters Directorate Ottawa, Canada, pp. 32-70.
- Meyers, G.D. (1992).** A Review of Nuclear Logging. *The Log Analyst* 33(3), pp. 228 – 238.
- Michalski, A. (2007).** Application of Temperature and Electrical Conductivity Logging in Groundwater Monitoring. *Groundwater monitoring and remediation.* 9 (3), pp. 112-118. doi:10.1111/j.1745-6592.1989.tb01158.x
- Molz, F.J. and Young, S.C. (1993).** Development and Application of Borehole Flowmeters for Environment Assessment. – *The Log Analyst* 34(1), pp. 13 – 23.
- National Research Council. (1996).** *Rock Fractures and Fluid Flow; Contemporary Understanding and Applications*, Natl. Acad. Press, Washington, D. C.
- Nicholl, M.J., Rajaram, H., Glass, R.J. and Detwiler, R. (1999).** Saturated flow in a single fracture: Evaluation of the Reynolds equation in measured aperture field. *Water Resour. Res.* 35, pp. 3361-3373.

**Nyende, J., Gomo, M. and van Tonder, G. (2014).** A Comparative Hydrogeochemical Study of Granitic Fractured and Alluvial Channel Aquifer Systems. *Int. J. Environ. Sci. Toxic. Res.* 2(3), pp. 64-80.

**Pacome, A.D. (2010).** Fracture characterisation of Karoo aquifers. MSc thesis. Institute for Groundwater Studies. Faculty of Natural and Agricultural Sciences. University of the Free State, Bloemfontein, South Africa.

**Paillet, F.L, Cheng, C.H. and Pennington W.D. (1992).** Acoustic-waveform Logging-advances in Theory and Application. – *The Log Analyst* 33(3), pp. 239 – 258.

**Paillet, F.L. and Pedler, W.H. (1996).** Integrated borehole profiling methods for wellhead protection applications. *Eng. Geol.* 42 (2-3), pp. 155–165.

**Pedler, W.H. and Urish, D.W. (1988).** Detection and characterization of hydraulically conductive fractures in a borehole: the emplacement method. *Eos, Transactions, American Geophysical Union*, 69(44), pp. 1186.

**Pedler, W.H., Barvenik, M.J., Tsang, C.-F. and Hale, F.V. (1990).** Determination of bedrock hydraulic conductivity and hydrochemistry using a wellbore fluid profiling method. *Proceedings of the Outdoor Action Conference – 1990, NWWA*, pp. 39-53.

**Pedler, W.H., Head, C.L. and Williams, L.L. (1992).** Hydro-physical profiling: A new wellbore technology for hydro-geologic and contaminant characterization of aquifers, *National Outdoor Action Conference, National Ground Water Association, Las Vegas, Nevada*.

**Raven, K.G., Novakowski, K.S. and Lapcevic, P.A. (1988).** Interpretation of field tests of a single fracture using a transient solute storage model. *Water Resour. Res.* 24 (12), pp. 2019-2032.

**Reedy, O.C., Jardine, P.M., Wilson, G.V. and Selim, H.M. (1996).** Quantifying the diffusive mass transfer of nonreactive solutes in columns of fractured saprolite using flow interruption. *Soil Sci. Soc.* 60, pp. 1376-1384.

**Repsold, H. (1989).** *Well Logging in Groundwater Development.* – *International Contributions to Hydrogeology 9*; Verlag Heinz Heise, Hannover.

**Riemann, K. (2002).** Aquifer Parameter Estimation in fractured-rock Aquifers using a Combination of Hydraulic and Tracer Tests. PhD, Thesis. Faculty of Natural and Agricultural

Sciences, Department of Geohydrology at the University of the Free State, Bloemfontein, South Africa.

**Sahimi, M. (1995).** Flow and transport in porous media and fractured rock: from classical methods to modern approaches. VCH, Weinheim, Germany, pp. 482.

**Sauty, J.P. (1980).** An analysis of hydro-dispersive transfer in aquifers. *Water Resource Research*, 16(1), pp. 145-158.

**Sawyer, A.H., Cardenas, M. B. and Buttlers, J. (2012).** Hyporheic temperature dynamics and heat exchange near channel-spanning logs. *Water Resources Research* 48. W01529.

**Schweitzer, J.S., Grau, J.A. and Hertzog, R.C. (1988).** Precision and accuracy of short lived activation measurements for in situ geological analyses, *J. Trace Microprobe Techniques* 64, pp. 437–451.

**Shapiro, A.M. (2002).** Fractured-Rock Aquifers, Understanding an increasingly important source of water. Fact Sheet FS-112-02, U.S. Department of Interior, U.S. Geological Survey.

**Singhal, B.B. and Gupta, R.P. (2010).** Applied Hydrogeology of Fractured Rocks, pp. 139-154.

**Smits, A. R., Fincher, D. V., Nishida, K., Mullins, O. C., Schroeder, R. J. and Yamate, T. (1993).** 'In-situ Fluid Analysis as an Aid to Wireline Formation Sampling', 68th Ann. Conf., Soc. Petrol. Eng., SPE 26496.

**Spies, B. R. (1996).** Electrical and Electromagnetic Borehole Measurements: A Review. *Surveys in Geophysics*, 17, pp. 517-556.

**Tang, D.H., Frind, E.O. and Sudicky, E.A. (1981).** Contaminant transport in fractured porous media: Analytical solution for a single fracture. *Water Resour. Res.* 17 (3), pp. 555-564.

**Taylor, R.G., Tindimugaya, C., Barker, J.A., Barrett, M., Macdonald, D.M.J., Kulabako, R., Nalubega, M. and Edwardmartin, R. (2010).** Convergent radial tracing of viral and solute transport in gneiss saprolite. *Ground Water* 48 (2), pp. 284–294.

**Tsang C.F. and Neretnieks, I. (1998).** Flow channelling in heterogeneous fractured rocks. *Rev. Geophys.* 36, pp. 275-298.

**Tsang, C.F. (1991).** Coupled hydromechanical-thermochemical processes in rock fractures, *Rev. Geophys.*, 29 (4), pp. 537-551.

**Tsang, C.-F. and Doughty, C. (2003).** Multi-rate flowing fluid electric conductivity method. *Water Resour. Res.* 39 (12), pp. 1354–1362.

**Tsang, C.F., Hufschmeid, P. and Hale, F.V. (1990).** Determination of fracture inflow parameters with a borehole fluid conductivity profiling method. *Water Resources Research.* 26 (4), pp. 561–578.

**Van Tonder, G. and Vermeulen, D. (2005).** Groundwater borehole report at Paradys Experimental Farm, Bloemfontein. Rprt N: 2005/03/PDV (Fevrier). Institute for Groundwater Studies.

**Van Wyk, A.E. (1998).** Tracer Experiments in Fractured-Rock Aquifers. M.Sc. Thesis. Institute for Groundwater Studies. Faculty of Natural and Agricultural Sciences. University of the Free State, Bloemfontein, South Africa.

**Ward, S. H. (1980).** 'History of Geophysical Exploration- Electrical, Electromagnetic and Magne- totelluric Methods', *Geophysics* 45, pp. 1659-1666.

**Williams, J.H. and Johnson, C.D. (2004).** Acoustic and optical borehole-wall imaging for fractured-rock aquifer studies: *Journal of Applied Geophysics.* 55 (1-2), pp. 151-159.

**Witthüser, K.T. (2001).** Untersuchung zum Stofftransport in geklüfteten Festgesteinen unter besonderer Berücksichtigung der Matrixdiffusion. Ph.D Thesis, Department of Applied Geology, University of Karlsruhe, Germany.

**Witthüser, K.T. (2003).** Geology department, Pretoria University, South Africa, Personal communication.

**Wonik, T. and Hinsby, K. (2006).** Borehole Logging in Hydrogeology. In: Kirsch, R., Rumpel, H.-M., Scheer, W., Wiederhold, H.(eds): *Groundwater resources in buried valleys - a challenge for geosciences.* Leibniz Institute for Applied Geosciences. Hannover, pp. 107-122.

**Xu, Y., van Tonder, GJ., van Wyk, B., van Wyk, E. and Aleobua B. (1997).** Borehole dilution experiment in a Karoo aquifer in Bloemfontein. ISSN 0378-4738. *Water SA.* 23 (2).

**Zimmerman, M.D., Bennett, P.C., Sharp Jr, J.M., Choi, W. (2002).** Experimental determination of sorption in fractured flow systems. 58 (1-2), pp. 51-77. doi:10.1016/S0169-7722(02)00023-2.

## **ABSTRACT**

Fluid electrical conductivity (FEC) profiling is a simple and efficient technique used to determine properties such as flow rate, salinity and hydraulic characteristics such as transmissivity. The method is also commonly used to identify and locate high inflow zones intersected by a wellbore, from which groundwater samples can be collected for the purpose of water quality monitoring. Moreover, the identified inflow zones may be targeted for transport and hydraulic tests which may assist in the understanding of groundwater flow and solute mass transport properties of the subsurface. The method primarily involves profiling the FEC with depth in a borehole under either natural or stressed conditions, using a downhole Temperature Level Conductivity probe. Once the FEC tests are conducted and graphs are obtained, observations may be derived from the profiles. Zones where fluid flows into the borehole displays anomalies in the FEC profiles, which may be analysed to infer inflow rate and salinity of the individual fractures. The current challenge with the use of this method is that its application has not yet been studied in a controlled laboratory aquifer environment, in order to understand the typical FEC profile responses in aquifers of different structures and groundwater qualities. Furthermore, no guidelines have been developed to assist in the interpretation of FEC profiles under different hydrogeological conditions. In this study laboratory tests were conducted with the use of a physical model to investigate the evolution of FEC profiles associated with a contaminant plume, in a horizontal single-plane fractured rock aquifer system. To achieve this, two groundwater flow and transport conditions were simulated; one with freshwater flow and the other with saline (contaminated) water. Generally, two distinct profiles associated with a contaminant plume in a borehole drilled in a horizontal single-plane fractured rock aquifer were identified and conceptualised as (1) the conceptual background profile and (2) the conceptual elevated FEC profile. Essentially, within the conceptual background profile three distinct segments (zones) were noted, each which responded differently; the upper segment, transition zone and the lower segment. The conceptual elevated FEC profile was observed when a contaminant associated with increased FEC values reached the monitoring borehole; its anomaly is more or less pronounced (at the fracture position) depending on the stage of the contaminant plume within the system. These profiles were observed under a controlled laboratory environment and were also verified in the field. The profiles which were obtained in the field were comparable to those observed in the laboratory experiment thus increasing the confidence in the accuracy of the laboratory results.